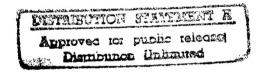
# NASA Technical Memorandum 110257



# Comparison of Separation Shock for Explosive and Nonexplosive Release Actuators on a Small Spacecraft Panel

M. H. Lucy and R. D. Buehrle Langley Research Center, Hampton, Virginia

J. P. Woolley Lockheed Martin, Sunnyvale, California



December 1996

19970630 098

National Aeronautics and Space Administration Langley Research Center Hampton, Virginia 23681-0001

# COMPARISON OF SEPARATION SHOCK FOR

# EXPLOSIVE AND NON-EXPLOSIVE RELEASE ACTUATORS ON A SMALL SPACECRAFT PANEL

# TABLE OF CONTENTS

ABSTRACT	1
1.0 SUMMARY	1
2.0 INTRODUCTION	1
3.0 TEST SETUP AND PROCEDURE	2
3.1 Release Mechanisms	2
3.2 Test Panel Configurations	3
3.2.1 Bare Panel Tests	3
3.2.2 Mass Simulator Tests	3
3.3 Release Device Mounting	3
3.4 Preload	3
3.5 Accelerometer Locations and Types	3
4.0 DATA ACQUISITION AND PROCESSING	4
4.1 Shock Measurements.	4
4.1.1 Time-Histories.	4
4.1.2 Shock Response Spectra	4
4.2 Impedance Measurements	
5.0 DISCUSSION OF RESULTS	5
5.1 Shock Responses	
5.1.1 Mass Loaded Panel Configuration (OEA, Hi-Shear 8mm and, 1/2-inch,	6
G&H and Martin Concept)	
5.1.1.1 Representative Response Levels	6
5.1.1.2 Comparison of Effects of Preload Level for the Martin Concept	7
5.1.1.3 Comparison of Levels from Different Release Devices	7
5.1.2 Bare Panel Configuration (OEA, Hi-Shear 1/2-inch and G&H Devices)	
5.1.2.1 Representative Response Levels	8
5.1.2.2 Comparison of Levels from Different Release Devices	8
5.1.3 Comparison of SRS Levels with the Bare and Mass Loaded Panel	8
5.2 Impedance and Transfer Functions.	
6.0 CONCLUSIONS AND RECOMMENDATIONS	
7.0 ACKNOWLEDGMENTS	
TABLE 1 CRSS Radial Panel Development Pyro Shock Tests	
FIGURES.	
APPENDIX A, Data Tables A -I Through III	36

#### COMPARISON OF SEPARATION SHOCK FOR EXPLOSIVE AND NON-EXPLOSIVE RELEASE ACTUATORS ON A SMALL SPACECRAFT PANEL

#### ABSTRACT

Functional shock, safety, overall system costs, and emergence of new technologies, have raised concerns regarding continued use of pyrotechnics on spacecraft. NASA Headquarters-Office of Chief Engineer requested Langley Research Center (LaRC) study pyrotechnic alternatives using non-explosive actuators (NEAs), and LaRC participated with Lockheed Martin Missile and Space Co. (LMMSC)-Sunnyvale, CA in objectively evaluating applicability of some NEA mechanisms to reduce small spacecraft and booster separation event shock. Comparative tests were conducted on a structural simulator using five different separation nut mechanisms, consisting of three pyrotechnics from OEA-Aerospace and Hi-Shear Technology and two NEAs from G&H Technology and Lockheed Martin Astronautics (LMA)-Denver, CO. Multiple actuations were performed with preloads up to 7000 pounds, 7000 being the comparison standard. All devices except LMA's NEA rotary flywheel-nut concept were available units with no added provisions to attenuate shock. Accelerometer measurements were recorded, reviewed, processed into Shock Response Spectra (SRS), and comparisons performed. For the standard preload, pyrotechnics produced the most severe and the G&H NEA the least severe functional shock levels. Comparing all results, the LMA concept produced the lowest levels, with preload limited to approximately 4200 pounds. Testing this concept over a range of 3000 to 4200 pounds indicated no effect of preload on shock response levels. This report presents data from these tests and the comparative results.

#### 1.0 SUMMARY

Concerns arising from continued use of pyrotechnics on spacecraft led NASA Headquarters-Office of Chief Engineer to request Langley Research Center (LaRC) form a Pyrotechnic Alternatives Investigative Team. In February 1995 LaRC was invited to cooperatively participate with LMMSC in evaluating actuation shock produced by several pyrotechnic and non-pyrotechnic release devices. The tests would objectively investigate application of some non-explosive actuators (NEAs) to reduce small spacecraft and booster separation event shock by demonstrating NEA release mechanisms, comparing resulting levels with those from standard pyrotechnic devices, and evaluating effects of a different test panel mounting arrangement.

Tests were conducted at LMMSC on a structural simulator representing a current small spacecraft panel design—with and without mass loading. Five different release mechanisms were tested in multiple firings with preloads ranging from about 3000 to 7000 pounds, the latter being the comparison standard. With the exception of a LMA rotary flywheel-nut developmental NEA device, hereafter referred to as the Martin concept, all other separation devices were available, off-the-shelf units with no additional provisions to attenuate functional shock.

Accelerometer measurements were made on the panel face and frame, acceleration-time histories reviewed for validity, valid data processed into Shock Response Spectra (SRS), and the SRS data compared. As expected, comparisons for standard preloaded (7000 pound) release mechanisms indicated the most severe levels were produced by the pyrotechnic devices, while the G&H NEA device produced the lowest levels. The Martin concept clearly produced the lowest levels, but its maximum preload capability was limited to approximately 4200 pounds. However, results from testing this developmental device, where the preload range was 3000 to 4200 pounds, indicated there was no systematic effect raising shock levels with preload.

Panel in-plane strain energy release was found to significantly raise the in-plane SRS levels compared to those in the direction normal to the panel face. Normal direction levels were influential at low frequencies, but in-plane levels clearly dominated at frequencies above 600 to 800 Hz. This result was not device dependent, although some spectral differences were noted between the pyrotechnic and NEA devices. Impedance and transfer function data support consistency of the SRS directional response evaluations. This latter data should prove useful in translating these test results to other structures, providing similar data are available on those structures.

#### 2.0 INTRODUCTION

Due to concerns arising from continued use of pyrotechnics on spacecraft, NASA Headquarters-Office of Chief Engineer, requested LaRC form a Pyrotechnic Alternatives Investigative Team. Reasons for this request included: high functional (actuation) shock levels; overall system costs; reusability; shrinking volume, weight and power budgets on smaller spacecraft; emergence and availability of new technologies; potentially hazardous nature of the materials involved; and several recent anomalies in which pyrotechnics could be suspect. Because of this activity, in February 1995, LaRC was invited to participate in a cooperative, cost sharing effort with LMMSC to evaluate functional shock produced by several pyrotechnic and non-pyrotechnic release devices. Consequently, LaRC initiated Task 31, "Low-Shock Booster Release

System Engineering Feasibility Demonstration" under Contract NAS1-19241, "Mission Systems & Operations Analyses of NASA Space Station Freedom Advanced Concepts".

Limited data exist for determining component exposure to shock from payload separation devices on lightweight-rigid structures characteristic of current generation, commercial sized spacecraft. Release devices used on previous spacecraft structures are expected to produce shock levels above those for which many standard components have been qualified. A current LMMSC spacecraft, Commercial Remote Sensing Satellite (CRSS), employs separation devices mounted so a major portion of the strain energy released upon separation is in the mounting plane of some major components. Most current experience is with mounting release devices on external brackets, which convert release motion into transverse bending waves before the shock reaches most components of interest. Together, these situations provided a strong motivation to obtain test data for the LMMSC mounting configuration using current separation devices and prospective devices that promise to produce lower component shock levels. A shock test program was devised and carried out to obtain such data.

The Task's purpose was to objectively investigate application of some NEAs to reduce small spacecraft and booster separation event shock levels. The primary goal was to demonstrate NEA mechanisms for release functions, and determine severity and compare resulting shock levels with those produced by standard pyrotechnic devices. A secondary goal was to evaluate effects of the different release device panel mounting arrangement. LMMSC's initial planning included developing math models, making analytical shock predictions, comparing test results with predictions, and correlating results with the math models. Program resources and schedule precluded development of math models.

The resulting shock test program provided data from five different separation devices (all essentially separation nut designs) mounted as indicated (Figure 1) on a model of the CRSS Radial Panel. This panel was configured with mass simulators representing one of the more heavily loaded CRSS panels. Tests were also performed using three of the release devices on the same panel in a bare configuration (no mass simulators). The standard preload released in the tests was 7000 pounds, as measured by a load cell washer under the restraining bolt head. However, two of the devices tested were incapable of achieving this preload level. One of these, the Martin concept, showed considerable promise for producing low shock levels. To assess its shock level variation with preload, a range of preloads from 3000 to 4200 pounds was used for this device. Shock acceleration response level data were recorded at various points on the panel for each device actuated.

Additional tests were performed to measure release device input mounting impedance and installed accelerometer mounting block transfer functions. Such measurements are intended to aid in extrapolating the included test measurement results to other mounting and structural configurations. A detailed description of the test setup and procedure is provided as a further aid in interpreting test results. One possible method for performing such an extrapolation is described in Reference 1<sup>1</sup> which resulted from work performed on NASA contract NAS5-29452 as reported in Reference 2<sup>2</sup>.

## 3.0 TEST SETUP AND PROCEDURE

#### 3.1 Release Mechanisms

Five different release mechanisms, immediately available from several sources, were tested on a single test panel. Mechanisms ranged from state-of-the-art pyrotechnics (OEA [Ordnance Engineering Associates]-Aerospace 3/8-inch diameter and Hi-Shear Technology Corporation 8mm and 1/2-inch diameter standard separation nuts--figure 2) to NEA designs (G&H Technology, Incorporated and Martin concept rotary flywheel-nut 3/8-inch diameter separation devices--figure 3). To obtain meaningful data, multiple firings of each device were conducted.

With the exception of the Martin concept, all other separation nuts were available, off-the-shelf units with no additional provisions to attenuate actuation shock. The Martin concept (currently under patent disclosure) was an engineering feasibility demonstration unit. Fundamentally it consisted of a housing containing a multi-start, coarse threaded bolt, rotary nut, and locking mechanism. It was fully reusable, required minimal actuation energy, and functioned in less than 50 msec. Exclusive fabrication rights for the Martin concept are held by Starsys Research Corporation of Boulder, CO where the concept, now referred to as the Fast Acting Shockless Separation Nut (FASSN), is undergoing further development as a flight-weight unit. Under their Advanced Release Technologies Satellite (ARTS) II Program, the Naval Research Laboratory, Naval Center for Space Technology, Washington, DC is currently evaluating FASSN in a 1/2-inch diameter size with a preload capability of 10,000 to 13,000 pounds. Eventually Lockheed Martin plans to evaluate a similar device and may investigate a 1-inch diameter sized FASSN in the 50,000 to 70,000 pound preload category.

<sup>&</sup>lt;sup>1</sup> NASA CR-183480; Shock Prediction Technology: Pyroshock Source Characteristics Study; S.L.Hancock, J.H.Shea, G.R.Dunbar, P.Chao, and A.W.York.

<sup>&</sup>lt;sup>2</sup> NASA CR-183479; Shock Prediction Technology: Technical Manual; Y.A.Lee, D.R.Crowe, W.Henricks, and D.M.Park.

#### 3.2 Test Panel Configurations

Tests were conducted at LMMSC on a structural simulator (Figure 1) representing a proposed Lockheed Martin Launch Vehicle (LMLV) CRSS Radial Panel—with and without mass loading. This panel was considered representative of a current small spacecraft design. The test unit consisted of a flat 1.5-inch thick honeycomb rectangular panel with overall dimensions of approximately 19-inches by 38-inches. The test unit was suspended by two bungee cords and prevented from excessive swinging by a third bungee attached to the bottom. Y orientation was perpendicular to the panel face, with X and Z in the plane of the panel.

The panel consisted of a honeycomb core, face sheets, and a frame. The honeycomb core was 4.5-pounds per cubic foot aluminum, and the face sheets were 0.032-inch thick 2024-T3 aluminum. The panel was framed by 0.080-inch 6061-T651 aluminum which formed a 1.5-inch wide channel with 1-inch legs. The face sheets were laid over and adhesively bonded to the 1-inch legs. The bottom cut-out (Figure 1) was the release interface site. This cut-out was framed by channel similar to that around the rest of the panel except the legs were 0.125-inch thick. The extension at the bottom of the cut-out frame, through which the release bolt passed, was a minimum of 5/8-inch thick aluminum. Tests were run in a bare panel configuration and in a configuration in which mass simulators were mounted to inserts through the panel face. Table 1 presents detailed conditions of all tests, devices tested, and the preload for each as determined by a load cell washer.

#### 3.2.1 Bare Panel Tests

Tests were run in the bare panel configuration for the OEA and G&H 3/8-inch, and the Hi-Shear 1/2-inch diameter devices. Due to limited availability of devices, only one test per device was run in the bare panel configuration.

#### 3.2.2 Mass Simulator Tests

Tests were conducted for all included separation devices with mass simulators attached to the panel. In general, three actuations were conducted for each device. However, the Martin concept was actuated seven times with preloads ranging from 3000 to 4200 pounds. Mass simulators were constructed of aluminum plate, having the same weight and footprint on the panel as the actual component. As shown on Figure 1, three simulators were used: two identical, 30-pound simulators were mounted on opposite sides of the panel; and a third 53-pound simulator was mounted nearer to the release interface.

#### 3.3 Release Device Mounting

Separation system mounting design for this panel (Figure 1) is somewhat unique as the majority of strain energy released upon device actuation is along directions in the plane of the panel. Of particular interest in these tests was the distribution of shock loads among the different directions for this mounting configuration. Such motion excites different modal groups than the more usual, bracket mounted release mechanisms. The latter tends to primarily excite panel bending modes where components are mounted, resulting in the dominant shock levels being oriented normal to the panel's surface.

The release interface was represented by a 1/2-inch thick steel plate, 10-inches square, representing the launch vehicle simulator as shown on Figure 1. When a release device was actuated, this plate fell away thereby producing no secondary contact with the test panel. Separation devices were mounted so the nut and catcher fell away with the steel plate, the bolt staying with the test panel. Additionally, bolts attaching the nut to the plate were loose so the nut separated from the plate by approximately 1/16-inch. Videotape recordings made of each test verified clean separation.

#### 3.4 Preload

The release devices had maximum preload capabilities ranging from about 3000 to 20,000 pounds. A 7000 pound preload was the comparison standard. In this Task, ranges of test parameters were minimized to obtain direct comparisons; however, based on bolt strength, the Hi-Shear 8mm pyrotechnically actuated separation nut was only capable of about 2700 pounds preload. The Martin concept was incapable of the desired preload. To help evaluate effects of preload, a series of tests were performed on the Martin concept in which only preload was varied. The remaining devices were tested at 7000 pounds preload. The load cell washer, from which preload was determined, was located under the bolt head on the panel side of the interface.

#### 3.5 Accelerometer Locations and Types

Data acquisition included 13 accelerometer measurements on the panel's outer frame edge, to which the release device was mounted. Additionally, 23 accelerometer data measurements were obtained on the panel face, where components would usually be mounted. These latter accelerometers were mounted and data recording arranged so that panel instantaneous directional response could be determined. Adequate frequency response up to 10 kHz was available.

The locations of various accelerometer blocks are shown on Figure 1. There were eight pyramid-shaped triaxial blocks and six wedge-shaped biaxial blocks. Each was configured to provide normal (Y) and unambiguous in-plane (X and Z) instantaneous accelerations for the surface on which they were mounted. The X and Z accelerations could be combined to yield an instantaneous in-plane resultant, which should represent the maximum in-plane acceleration amplitude experienced at the measurement location.

Different accelerometers were used on different blocks to accommodate the expected environment. Where the highest levels were expected, Endevco type 7755 accelerometers, with a frequency response of + or - 5 percent from 10 Hz to 10 kHz and a maximum range of 50,000 g, were used on blocks 1,3 and 4. These accelerometers had an 11 kHz mechanical filter to prevent high frequency, high level accelerations from corrupting lower frequency data. Endevco type 2255 accelerometers, with a frequency response of + or - 5 percent from 20 Hz to 20 kHz and a maximum range of 20,000 g, were used on block 2. Endevco type 7250 accelerometers, with a frequency response of + or - 5 percent from 3 Hz to 20 kHz and a maximum range of 5,000 g, were used on the remaining blocks (pyramid blocks 5 through 8 and wedge blocks 9 through 14).

Accelerometers in locations 1 through 8 were mounted in a triaxial configuration on the pyramid-block mounts. The pyramid mounts were geometrically designed to co-locate the three accelerometer sensitive axes at the specimen surface (block mounting face). Locations 9 through 14 were mounted in a biaxial configuration using the wedge-block mounts. The wedge mounts also geometrically positioned the two accelerometers to produce co-incident sensitive axes at the specimen surface.

## 4.0 DATA ACQUISITION AND PROCESSING

#### 4.1 Shock Measurements

The CRSS panel release mechanism shock measurement data were recorded using LMMSC's acoustic real-time data acquisition system for vibration and acoustic testing. The system is composed of accelerometer transducers, signal conditioning, anti-alias filters, digitizing and storage components. The signal digitization was performed at 50,000 samples per second with a resolution of 14 bits (1 in 16384).

#### 4.1.1 Time-Histories

Basic shock data were recorded in the form of acceleration-time histories. Accelerometer blocks were shaped so the time phased data could be combined to obtain resultant acceleration-time histories in any direction. Particularly, acceleration-time history in the direction normal to the block mounting surface, and at least one direction in the plane of this surface could be determined for each block. The pyramid block permitted resolution of acceleration into two orthogonal directions in the plane of its mounting surface, as well as into an instantaneous resultant acceleration in that plane.

Response acceleration-time histories were reviewed to determine individual measurement validity. Data determined to be valid was further processed into SRS. SRS were computed using a standard dynamic amplification factor (Q) of 10 (5 percent of critical damping). Data reduction was performed in stages to take advantage of existing LMMSC post-processor software. First, accelerometer responses from each mounting block were vector summed to produce acceleration resultants in the three primary panel axes (X-Y-Z for the pyramid and Y-Z or X-Z for the wedge). These resultants were stored in ASCII data files, one per block-panel axis. Data from positions 1 through 8 were also vector summed to produce the in-plane (X-Z plane) resultants. Finally, the ASCII data were input to the SRS post-processor to produce the SRS output and plot data files.

Typical X-,Z- and Y-direction acceleration-time histories are shown on Figures 4 and 5. These are typical of results obtained from resolving pyramid block data into orthogonal components. Similar results were produced by such resolution of the two-dimensional wedge blocks. Figure 4 is an acceleration-time history taken from a test of the G&H NEA separation nut. Figure 5 is similar data taken from a test of the Martin concept. Exclusive of the maximum levels indicated, the first figure is more typical of separation nut acceleration-time histories (explosive or NEA) in that there is only a single pulse associated with release. Data from the Martin concept, shown in Figure 5, exhibits three distinct pulses, indicative of extended and multiple actions involved in the release process for this mechanism.

#### 4.1.2 Shock Response Spectra

The ASCII data files were read into the processor, the anti-alias (11.2 kHz) filter transfer function was analytically removed and a six pole, 10 Hz AC coupling was performed. The SRS was generated from 100 to 10,000 Hz with 1/6th-octave filters. Positive, negative and noise floor SRS were computed. Files were also generated containing the time-history and envelope of the SRS.

#### 4.2 Impedance Measurements

A series of tests to characterize dynamic behavior of the CRSS panel when subjected to pyrotechnic inputs was performed. These "tap" tests were performed using a Kistler instrumented hammer with an integral, calibrated load cell to tap on a bolt representing the release device bolt. A special hard tip was used to provide significant energy up to 10 kHz. An accelerometer placed on this bolt and the hammer's load cell enabled determination of an input impedance. The same accelerometers and locations as shown in Figure 1 were used throughout the release tests, but the mass simulators were removed. The response of these accelerometers were recorded during the tap tests to determine the transfer function relating their response to a general input excitation. A series of measurements were taken with the 3/8-inch diameter pyrotechnic-attachment point configuration. Then the hole was drilled to accept the 1/2-inch diameter pyrotechnic device, and another series of measurements taken.

The tests were performed by first, attaching a steel block (1.25-inch cube) at the panel's release device attachment point. The block was attached by first a 3/8- and later a 1/2-inch bolt, respectively, for the two series of tests. Excitation was provided by impacting the steel block with the instrumented hammer at approximately 1-second intervals for about 30 seconds. In addition to the accelerometers mounted on pyramid and wedge blocks that were used for the release tests, three accelerometers were mounted as close as possible to the impact point:

- a. A Z-accelerometer was mounted at the top of the block-attachment bolt.
- b. An X- and Y-accelerometer were mounted on the impact block opposite the impact point (refer to Figure 1 for the axis orientations).

These accelerometers, called "foot" accelerometers, were intended to yield data representing the mounting point impedance for this panel. Similar data for another installation should make the present results transferable.

The acceleration- and force-time histories were acquired by the LMMSC real-time data acquisition system. The data acquisition rate was 30,000 samples per second and 8-pole, 11.2 kHz, Butterworth, low-pass (anti-alias) filters were used. The impact levels were nominally 1500 pounds but varied between approximately 800 and 1900 pounds. Data analysis was performed with the signal analysis processor. The procedure was:

A peak detection system was used on the force-time histories to determine when impacts occurred. Exactly 2048 points were selected around each impact. Each time-history was inspected to assure there was a pre-trigger of at least 256 points and that there was only a single impact within the range of sample points. Response data from up to ten of the responses was retrieved for all "acceptable" time windows.

Transfer functions between responses and force input were calculated for each impact. These transfer functions were then averaged (using ten averages for the "3/8-inch bolt" test and at least seven averages for the "1/2-inch bolt" test).

The 1/6th-octave impedance was calculated from the transfer functions by:

- 1. Calculating the acceleration impulse function via inverse Fast Fourier Transform (FFT).
- 2. Subtracting off the average offset (AC coupling).
- 3. Multiplying by 386.4 to convert from a "g" calibration to inches/second/second.
- 4. Integrating to obtain the velocity impulse function.
- 5. Calculating the velocity transfer function by forward FFT.
- 6. Calculating the impedance by complex inversion of the velocity transfer function.

Determination of the 1/6th-octave impedance spectrum was completed by averaging the magnitude of the impedancespectral components over each 1/6th-octave band. The same 1/6th-octave center frequencies were used for these calculations as for the SRS calculations.

#### 5.0 DISCUSSION OF RESULTS

Overall measures of SRS produced by the devices were derived from the data and compared for accelerometers located on the panel face. Comparisons indicated the most severe levels were produced by the OEA device, followed by the Hi-Shear 1/2-inch diameter device. Of the devices capable of 7000 pound preload, the G&H NEA device produced the lowest levels. In these tests the Martin concept clearly produced the lowest levels, but its maximum preload capability was limited. Of the devices tested, LMMSC selected the Hi-Shear 1/2-inch diameter separation nut for further consideration. A comparison of results from the Martin concept for several preloads indicated there was no systematic effect of rising preload causing an increase in shock levels over the range tested. Such a result may eventually break down at some higher level of preload.

In-plane strain energy release was found to significantly raise the shock environment in-plane SRS levels compared to the normal direction levels. It was still found that the normal direction levels were influential at low frequencies, but in-plane levels were clearly dominant in the higher frequencies (above 600 to 800 Hz). This result was not device dependent, although some spectral differences can be noted between the pyrotechnic devices and NEAs. The SRS generally showed an increase with frequency, with only levels and local details varying with device. The panel's dynamic properties probably provide the dominant aspect to determining spectral shapes with the devices all providing broad band excitation, differing primarily in level only.

Impedance and transfer function data taken support the consistency of the SRS directional response evaluations. This data should prove useful in translating the test results contained herein to other structures, providing similar data are available on those structures. Comparative data used in this report are tabulated in Appendix A.

#### 5.1 Shock Responses

SRS were determined for five different separation devices with the CRSS panel in the mass loaded configuration and for three different devices with the panel in the bare (unloaded) configuration. Data were resolved into normal (Y-axis) and in-plane (X- and Z-axis) as well as in-plane instantaneous resultant magnitude, before the SRS were calculated. The SRS were computed for each orthogonal axis and in-plane resultant, where such data were available, using the standard Q of 10. SRS data were subjected to statistical analysis using various groupings to obtain comparisons for the differences between devices and test condition effects.

Although data were taken and reduced to SRS form on the frame, only data from the face sheets were used in the analyses. It was anticipated that shock propagation in this panel, with the type of mounting used for the separation devices, would have been rather complex. The frame data were taken to enable the study of shock propagation for the panel in the event these complexities actually appeared. The test results did not indicate that such studies were warranted or necessary, so they were not performed. Only the non-frame, flat panel data are treated herein. These data represent the environment of panel mounted components.

#### 5.1.1 Mass Loaded Panel Configuration (OEA, Hi-Shear 8mm and 1/2-inch, G&H and Martin Concept)

Data from all five separation devices were taken for the test panel configured with mass simulators. At least three tests were performed with each device for this panel configuration. Twenty-three accelerometer channels on the panel face were recorded for each test. The standard preload for these tests was 7000 pounds, as indicated by the load cell instrumentation. Two of the devices, the Hi-Shear 8mm device and Martin concept, were not capable of the standard preload. They were loaded to the maximum permissible preload, which was about 2700 pounds for the Hi-Shear 8mm device; and the Martin concept was tested over a range of preloads from 3000 to 4200 pounds, as indicated in Table 1. Assimilation of this mass of data into an interpretable form was the first order of the analysis process. A statistical approach was used for this purpose.

#### 5.1.1.1 Representative Response Levels

Data from any one grouping of measurements was assumed to behave as a log-normal random variable. Various axis groupings were constructed and log-normal statistical properties of these groups were compiled and compared. The groups were: acceleration normal to the panel surface (Y-axis, designated as nfy); orthogonal in-plane (X- and Z-axes, designated as nfxz); in-plane resultant (of X and Z components, designated as nfip); and combined normal and in-plane resultant levels. In computing the statistical properties, no segregation by location on the panel face was included. Nomenclature used includes; nf (no frame), and i or ip (in-plane). Figures 6 (a) through (e) show the comparisons of data groupings 95th percentile levels for each device and preload:

- (a) OEA 3/8-inch diameter pyrotechnic separation nut, 7000 pound preload.
- (b) Hi-Shear 1/2-inch diameter pyrotechnic separation nut, 7000 pound preload.
- (c) G&H 3/8-inch diameter NEA separation nut, 7000 pound preload.
- (d) Hi-Shear 8mm diameter pyrotechnic separation nut, 2700 pound preload.
- (e) Martin 3/8-inch diameter concept, 4000 and 4200 pound combined preload.

Figures 7 (a) through (e) show the same sequence of device results, but compare the maximum measured level in each grouping.

In both sets of above figures, it may be seen that the combined normal and in-plane resultant levels serve as a reasonable indicator of an upper bound level. The upper bound level is always this combination for the maximum measured levels of

Figures 7. This must be true because the in-plane resultant is greater than or equal to the X- or Z-direction maxima and the combined maximum bears the same relation to the normal and in-plane directions.

If the reader seeks differences in the directional SRS levels, it may be observed that the normal direction is somewhat more influential in the lower frequencies and the in-plane motion dominates the higher frequencies. It is suggested by the impedance measurements, discussed later, that one might expect that panel modes associated with bending waves, which involve out-of-plane motion, come to bear at lower frequencies than the shear and longitudinal wave modes. The reader is cautioned that a resonant phenomenon is not involved here, but when the transient motion produced by the release is spectrally resolved, the natural modes of the system will indicate pronounced motion in their frequency bands.

A few instances were noted where the X-Z direction maximum measured level appeared to exceed the in-plane resultant level. These were found to be instances where there had been a zero shift in the accelerometer calibration during the test. This shift was not apparent for the X- or Z- measurements alone, whereas it was for the in-plane measurement. The data had been eliminated from consideration in the latter and not the former and thereby caused the faulty indication. Inspection of the time-histories of the original data confirmed in all cases that the data were faulty when there was a difficulty of this nature.

Figures 8 (a) through (e) show the relation between the arithmetic mean, the log mean, the 95th percentile and the maximum measured levels for the same sequence of devices. The difference between the log mean and the 95th percentile is indicative of the standard deviation for the data. These data, the standard deviation, sample size and Gumbel Factor (a correction for statistical errors due to small sample size) are presented in tabular form in Appendix A, Table A-1, (a) through (e), for the same sequence of devices.

There is close correspondence between the maximum measured and 95th percentile levels. It may be seen from these figures that the maximum measured level is the upper bound of the 95th percentile at all but a few frequency ranges of relatively narrow extent. Further, exceedances in these frequency ranges are of relatively small extent. These facts indicate there is little data scatter. Since data were collected from the entire panel face, this indication reveals there is little spatial variation of the shock levels over the panel face.

#### 5.1.1.2 Comparison of Effects of Preload Level for the Martin Concept

The Martin 3/8-inch diameter NEA concept was incapable of achieving the standard preload. It was tested over a range from 3000 to 4200 pounds. To assess effects of preload on results, these measurements are compared with one another. Combined normal and in-plane resultant levels are used as the basis for this comparison. Statistical features of these measurements are given in Appendix A, Table A-1, (e) through (i), for:

- (e) Combined 4200 and 4000 pound preload
- (f) 4200 pound preload
- (g) 4000 pound preload
- (h) 3500 pound preload
- (i) 3000 pound preload

The 95th percentile and maximum levels are shown in Figures 9 (a) and (b), respectively. The reader should note there is no clear trend associated with preload magnitude, as maximum measured SRS levels for 3000 pound are as great as those for the 4200 pound preload. Interpretation of the 95th percentile data is somewhat more difficult due to the small sample size producing more erratic indications.

#### 5.1.1.3 Comparison of Levels from Different Release Devices

The SRS 95th percentile and maximum levels are compared for all devices as measured with the maximum preload achieved for that device. These are shown in Figures 10 (a) and (b), respectively. The ordering of levels for the different devices is the same for both the 95th percentile and maximum measured levels. The order from higher to lower levels is: OEA; Hi-Shear 1/2-inch; Hi-Shear 8mm; G&H; and the Martin concept. The Martin concept produced levels significantly lower than the others; however, its greatest preload was only 4200 pounds as compared to 7000 pounds for the OEA, Hi-Shear 1/2-inch and G&H devices. Such a difference in preloads could make a significant difference in the shock levels produced, although its variation over the range tested did not indicate a strong dependence on this parameter.

#### 5.1.2 Bare Panel Configuration (OEA, Hi-Shear 1/2-inch and G&H devices)

Tests were performed using OEA, Hi-Shear 1/2-inch and G&H devices at a preload of 7000 pounds with the test panel devoid of mass simulators. Due to limited availability of release devices, it was possible to perform only one test for each

OEA and Hi-Shear 1/2-inch device with the panel in this configuration; however, three tests were performed with the G&H device. A similar procedure was followed for evaluating data from the bare panel tests as was done for the panel with mass simulators.

#### 5.1.2.1 Representative Response Levels

SRS acceleration levels measured on the panel face were grouped in the same axis directions as previously done for the mass simulator data. As before, these groups were subjected to statistical analysis. The 95th percentile data are compared in Figures 11, and Figures 12 for the maximum measured levels with data for the individual devices presented separately in the (a), (b) and (c) versions of these Figures, as follows:

- (a) OEA 3/8-inch diameter pyrotechnic separation nut.
- (b) Hi-Shear 1/2-inch diameter pyrotechnic separation nut.
- (c) G&H 3/8-inch diameter NEA separation nut.

The combined normal and in-plane directions grouping is again considered to best represent the levels produced by each device. However, results are not as clear as before because of the significantly smaller sample sizes in the measurements.

Figures 13 (a) through (c) show the relation between the arithmetic mean, log mean, 95th percentile and maximum measured levels for the same sequence of devices in the bare panel configuration. The difference between the log mean and 95th percentile is indicative of the standard deviation for the data. These data, the standard deviation, sample size and Gumbel Factor are presented in tabular form in Appendix A, Table A-II, (a) through (c), for the same sequence of devices.

Because of the small number of measurements, the 95th percentile levels are frequently greater than maximum measured levels for this series of tests of the OEA and Hi-Shear 1/2-inch devices. This is not the case for the G&H device, since three tests were performed with it in the bare panel configuration.

#### 5.1.2.2 Comparison of Levels from Different Release Devices

SRS acceleration levels from the three devices were compared by means of results from the combined normal and in-plane resultant measurements. Figure 14 (a) and (b) show comparisons between their 95th percentile and maximum measured levels, respectively. The relative levels, as indicated by either the 95th percentile or maximum measured SRS accelerations, indicate the highest output from the OEA device, followed by the Hi-Shear 1/2-inch diameter and G&H device, respectively. However, there appears little difference between the last two devices for these bare panel tests as compared to their relative levels for the panel with mass simulators (refer to Figures 9). The paucity of measurements for the Hi-Shear device in the bare panel configuration is probably a major factor in this apparent difference. It is likely that both the OEA and Hi-Shear device levels are inaccurately represented by the small sample size. Such likelihood is reinforced by the results obtained by comparing the bare and mass loaded panel SRS levels produced by these devices.

# 5.1.3 Comparison of SRS Levels with the Bare and Mass Loaded Panel

Data representative of the SRS acceleration levels produced by the three devices that were tested on both the bare and mass loaded panel were compared. Figure 15 (a) and (b) show the 95th percentile and maximum measured levels, respectively, for the OEA, G&H and Hi-Shear 1/2-inch devices. This is a replot of data previously presented for each.

The reader may note for the first two devices, there are large frequency bands in which levels for the mass loaded panel exceed those for the bare panel. One is tempted to conjecture by referring to Figure 1, that all accelerometers used in compiling the statistics are in positions that are unshielded by the mass simulators. Furthermore, they may well be the recipient of energy reflected from these simulator bodies, and one might expect higher response levels to be produced. However, data for the G&H device follow the accepted behavior, and indicate the bare panel levels consistently exceed those for the mass loaded panel, as physical reasoning would lead one to expect. Recall that data for the G&H device represent a statistical sample which includes three test actuations of the device for each configuration. The mass loaded data for the OEA and Hi-Shear devices also represent data from three actuations, but the bare panel levels represent data from only one actuation of each. This is an indication that relative levels of the bare and mass loaded panels are not of the same confidence level in representing the expected results from these two devices, whereas, those for the G&H device are.

## 5.2 Impedance and Transfer Functions

Impedance data were calculated for the "foot" accelerometers mounted near the separation device for the test performed with the 3/8-inch bolt. Data from the 1/2-inch bolt test were not as good (the hammer hits and resulting data were erratic), so they have not been reduced to 1/6th-octave results.

The 1/6th-octave "foot" impedances for the three orthogonal directions resulting from excitation in these X-, Z- and Y-directions are shown in Figures 16, 17 and 18, respectively. The plotted data are also tabulated in Appendix A, Table A-III (a) through (c). The first two of these directions lies in the plane of the panel, while the Y-direction is normal to this plane. The general shapes of the impedance curves are similar for the X- and Z-direction excitations and responses, being consistent with no modes associated with motion in these directions below about 600 Hz. The Y-direction excitation impedances exhibit a character indicating modes associated with motion in this direction (probably bending) beginning in the neighborhood of 300 Hz. As was mentioned in describing the SRS results, the Y- (normal) direction of motion seemed to have the greater influence in the low frequencies and the in-plane motion seemed to dominate the higher frequencies.

The "foot" data are intended to represent the mounting point impedance for this panel. Similar data for another installation should enable estimation of the shock input energy obtained in these tests to that of the other installation, given proper dynamic models. The transfer function data for other test panel accelerometer blocks will be useful in constructing and validating such models.

#### 6.0 CONCLUSIONS AND RECOMMENDATIONS

SRS results for accelerations on the face sheets, where components are mounted, were combined into axis groups and subjected to statistical analysis. It was found that variation of level over the panel face was relatively small, as indicated in the small standard deviation from the statistical analysis. Differences between normal and in-plane resultant levels were also small although some spectral differences were noted and are described below. A combination of these directional levels was found to fairly represent behavior of the individual devices, although there would be little qualitative difference noted in picking any of the groupings to represent a device.

Overall measures of shock levels (SRS's) produced by the devices were derived from the data and compared for accelerometers located on the panel face. These comparisons indicated the most severe levels were produced by the OEA device, followed by the Hi-Shear 1/2-inch diameter nut. Of the devices capable of 7000 pound preload, the G&H NEA device produced the lowest levels. The Martin concept clearly produced the lowest levels in the test series, but its maximum preload capability was only 4200 pounds.

A comparison of results from the Martin concept for preloads, from 3000 to 4200 pounds, indicated there was no systematic effect raising shock levels with preload for this device over the range tested. However, it is expected that such a result may break down at some higher level of preload or it may be only due to the small amount of data used.

In-plane strain energy release was found to significantly raise the in-plane SRS levels of the shock environment compared to the normal direction levels. It was still found that normal direction levels were influential at low frequencies, but in-plane levels were clearly dominant in the higher frequencies (above 600 to 800 Hz). This result is not device dependent, although some spectral differences can be noted between the pyrotechnic and NEA devices. The SRS trends showed an increase in level with frequency. The dynamic properties of the test panel probably provide the dominant aspect determining the spectral shapes with the devices all producing broad band excitation, differing primarily in level only.

Impedance and transfer function data taken support the consistency of SRS directional response evaluations. They are indicative of the presence of low frequency bending waves (beginning at about 300 Hz) and onset of shear and dilatation waves at the higher frequencies (600 to 800 Hz). This data should also prove useful in translating these test results to other structures, providing similar data are available on those structures.

Data used for comparison purposes in the report are tabulated in Appendix A which represent reduced test data.

#### 7.0 ACKNOWLEDGMENTS

This effort was principally performed under Contract NAS1-19241, Task 31, at LMMSC by James P. Woolley, and the LaRC Task Monitor was Melvin H. Lucy, assisted by Ralph D. Buehrle. The point-of-contact (POC) and device provider for the Hi-Shear 8mm pyrotechnic separation nuts was Richard G. Webster. The POCs, device providers and refurbishers for the G&H NEA stored mechanical energy separation nut were John Bielinski and Wayne Powell. The Martin concept was supplied by Bill Nygren from the LAM-Denver Division. The authors express their gratitude to several individuals who contributed to the successful outcome of this program. Special thanks are due LMMSC's Messrs. Strether Smith and William Hollowell for their aid in data acquisition, analysis and post processing, and for their contributions to those report sections. LMMSC's Messrs. Myron Leigh and David Kreuger, who operated the data acquisition system and conducted the test operations, respectively, are responsible for the excellent quality of the data obtained from these tests. Finally, the coordination efforts of Messrs. Mike Otvos and Marc Gronet of LMMSC who set the stage for a seamless effort by the several organizations involved.

Table 1 CRSS Radial Panel Development Pyro Shock Tests

Run No.	Test No.	Туре	Time/Date	Data File	Preload	Mass Sim	Video No.	Data Table
1	1	3/8 G&H	10:38 27-Mar	L858E01	7000	Yes	3	A-1 (c)
2	2	3/8 G&H	13:21 27-Mar	L858E02	7000	Yes	4	
3	3	3/8 G&H	14:15 27-Mar	L858E03	7000	Yes	5	
4	4	3/8 G&H	15:40 27-Mar	L858E04	7000		6	A-2 (c)
5	5	3/8 G&H	16:49 27-Mar	L858E05	7000		7	
6*		3/8 G&H	18:49 27-Mar		7000		8	
7	6	3/8 G&H	18:56 27-Mar	L858E06	7000		9	
8	7	8mm HiS	14:59 28-Mar	L858E07	2440	Yes	10	A~1 (d)
9	8	8mm HiS	10:30 31-Mar	L858E08	2670	Yes	11	
10	9	8mm HiS	14:40 31-Mar	L858E09	2600	Yes	12	
11	10	3/8 OEA	14:23 03-Apr	L858E10	7000	Yes	13	
12	11	3/8 OEA	10:54 12-Apr	L858E11	7000	Yes	14	A-1 (a)
13	12	3/8 OEA	13:30 12-Apr	L858E12	7000	Yes	15	
14	13	3/8 OEA	11:20 13-Apr	L858E13	7000		16	A-2 (a)
15**		1/2 HiS	15:00 17-Apr		7000		1	
16	14	1/2 HiS	09:38 18-Apr	L858E14	7000		18	A-2 (b)
17	15	1/2 HiS	14:00 18-Apr	L858E15	7000	Yes	19	A-1 (b)
18	16	1/2 HiS	10:24 19-Apr	L858E16	7000	Yes	20	
19	17	1/2 HiS	13:44 19-Apr	L858E17	7000	Yes	21	
20***		3/8 Martin	15:00 19-Apr		2700	Yes	22	
21	М1	3/8 Martin	10:23 20-Apr	L858M01	3000	Yes	23	A-1 (j) & (k)
22	M2	3/8 Martin	11:30 20-Apr	L858M02	3000	Yes	24	
23	МЗ	3/8 Martin	12:39 20-Apr	L858M03	3000	Yes	25	
24	M4	3/8 Martin	13:13 20-Apr	L858M04	3500	Yes	26	
25	M5	3/8 Martin	13:40 20-Apr	L858M05	4000	Yes	27	A-1 (e), A-1 (j) & (k)
26	M6	3/8 Martin	14:00 20-Apr	L858M06	4000	Yes	28	
27	М7	3/8 Martin	14:28 20-Apr	L858M07	4200	Yes	29	
	F1	X- Dir Tap						A-3 (a)
	F2	Z- Dir Tap						A-3 (b)
	F3	Y- Dir Tap						A-3 (c)

Wire came loose on firing system - no release, no accl data retained.

Note: 1) Because of inaccuracies of load washer, all preload values are approximate.

2) Impedance Test File Names: L858HAM1 thru HAM9. L858HAM4 thru HAM6 are retests of L858HAM1 thru HAM3.

<sup>\*\*</sup> Bolt Bottomed-out in sep nut - squib fired, no release, no accl data retained.

<sup>\*\*\*</sup> Preliminary release, no accl data recorded.

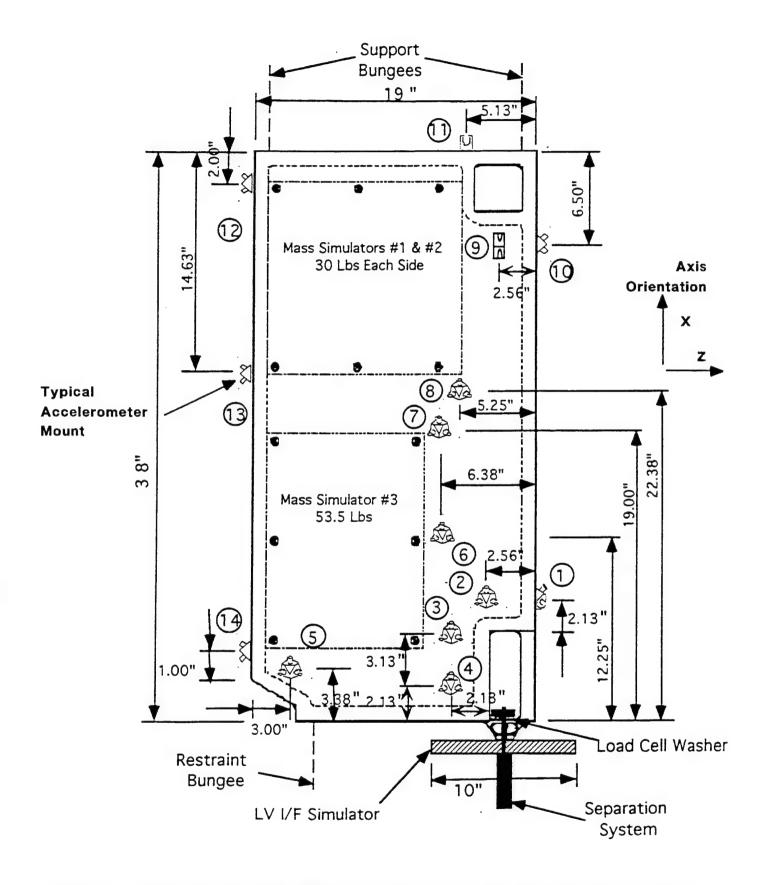


Figure 2. Test Panel with Masses and Accelerometer Block Locations.

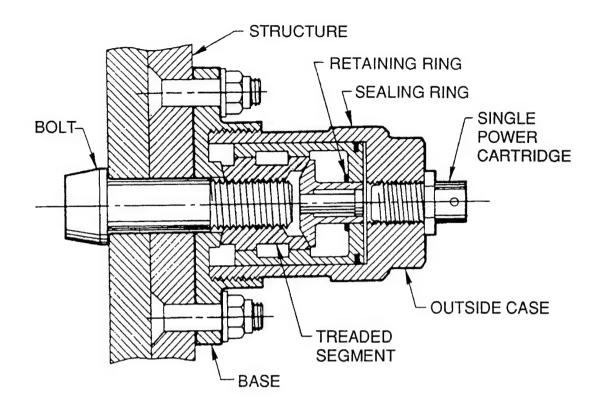


Figure 2. Typical Pyrotechnic Separation Nut (Hi-Shear Depicted).

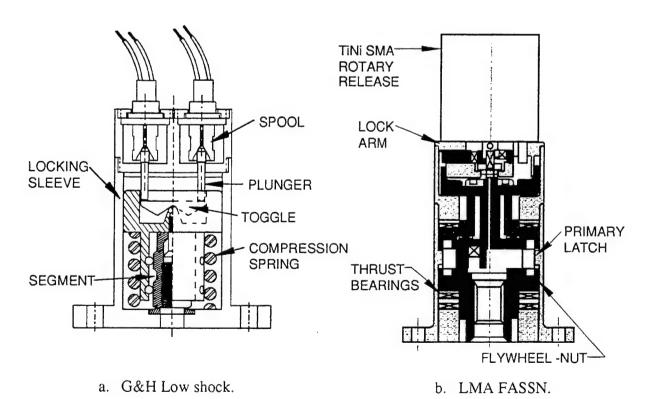
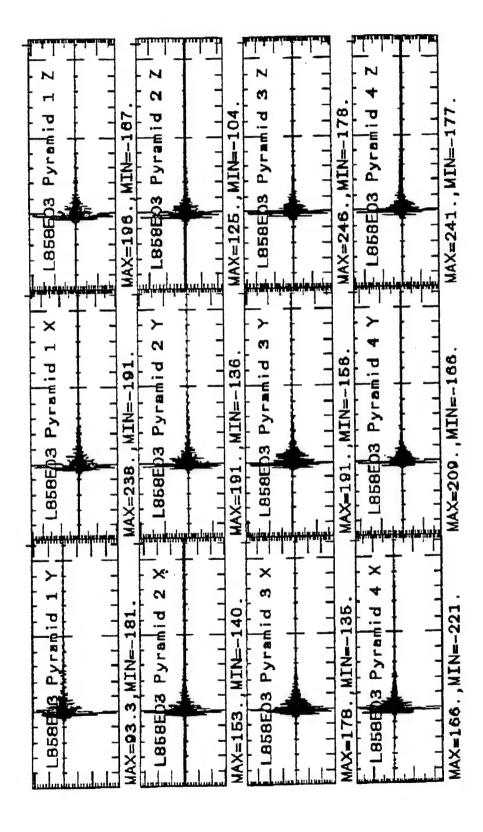


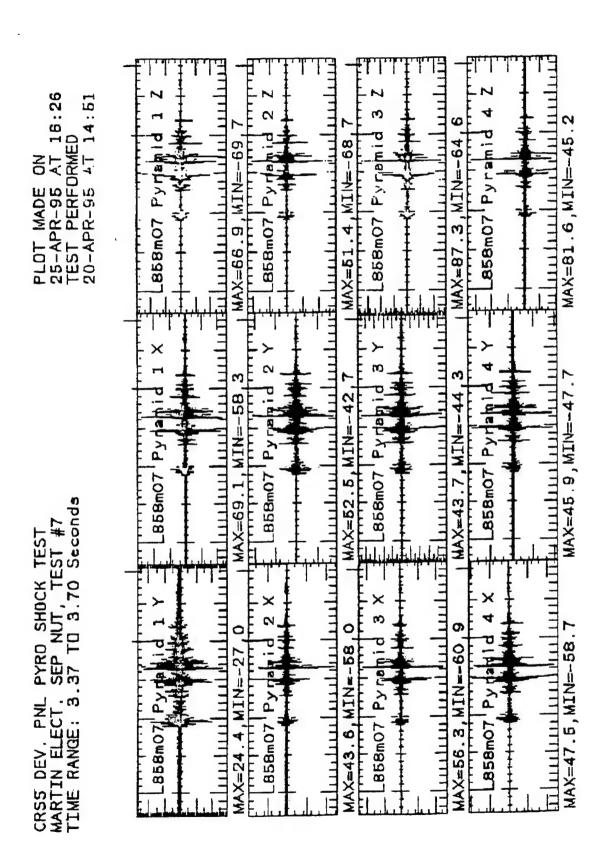
Figure 3. Non-Explosive Actuated Separation Devices.

CRSS DE. PNL PYRO SHOCK #3 GNH 3/8" NON-EXPLOSIVE TIME RANGE: 6.85 TO 7.01 Seconds

PLOT MADE ON 31-DEC-95 AT 16:21 TEST PERFORMED 27-MAR-85 AT 14:12



Typical X-, Y-, and Z-Direction Acceleration Time Histories from G&H Device. Figure 4.



Typical X-, Y-, and Z-Direction Acceleration Time Histories from Martin Device. Figure 5.

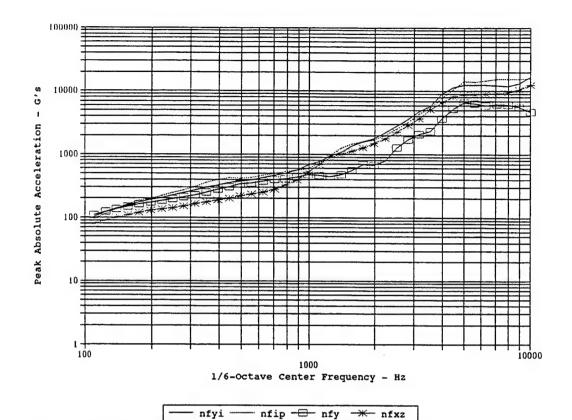


Figure 6(a). OEA 3/8", with Masses, 7000 lb., Various Axis Groupings, SRS (Q=10), 95th Percentile Levels.

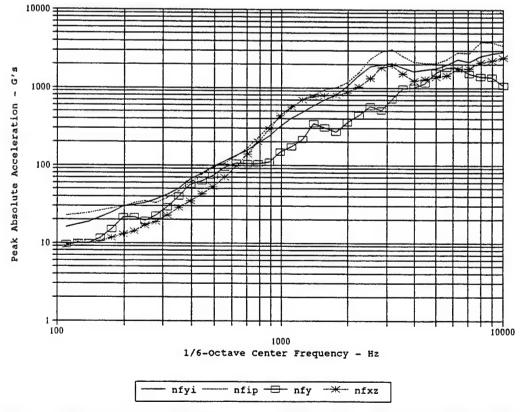


Figure 6(b). HiS 1/2", with Masses, 7000 lb., Various Axis Groupings, SRS (Q=10), 95th Percentile Levels.

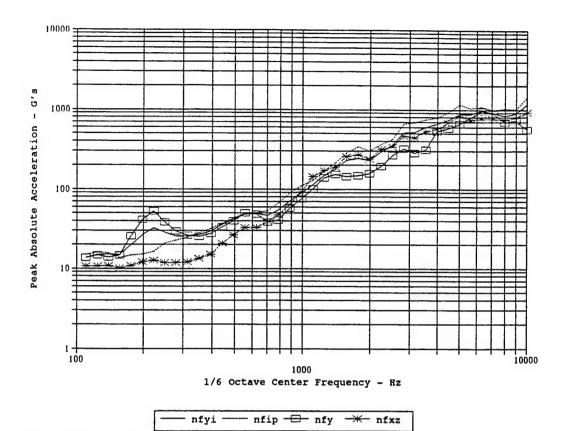


Figure 6(c). G&H 3/8", with Masses, 7000 lb., Various Axis Groupings, SRS (Q=10), 95th Percentile Levels.

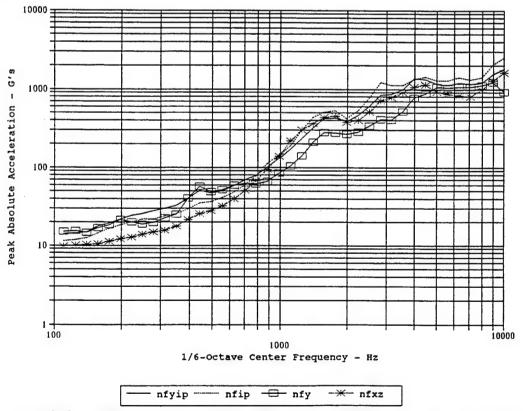


Figure 6(d). HiS 8 mm, with Masses, 2700 lb., Various Axis Groupings, SRS (Q=10), 95th Percentile Levels.

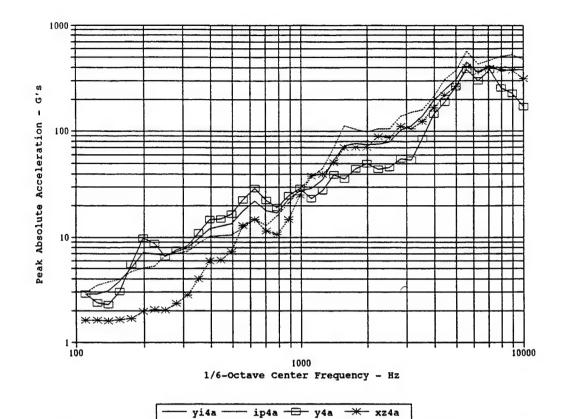


Figure 6(e). LM 3/8", with Masses, Combined 4000 & 4200 lb., Various Axis Groupings, SRS (Q=10), 95th Percentile Levels.

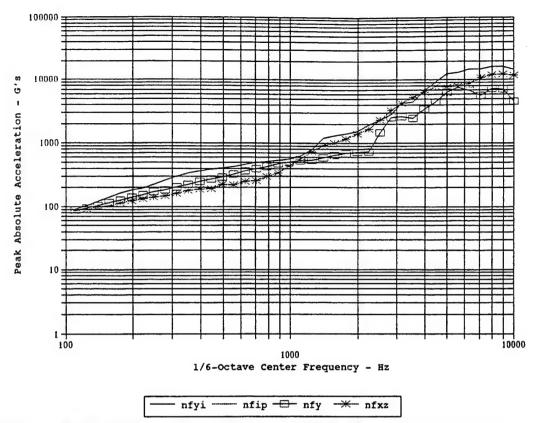


Figure 7(a). OEA 3/8", with Masses, 7000 lb., Various Axis Groupings, SRS (Q=10), Maximum Measured Levels.

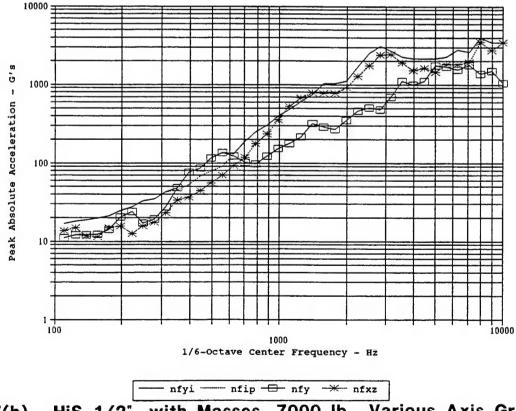


Figure 7(b). HiS 1/2", with Masses, 7000 lb., Various Axis Groupings, SRS (Q=10), Maximum Measured Levels.

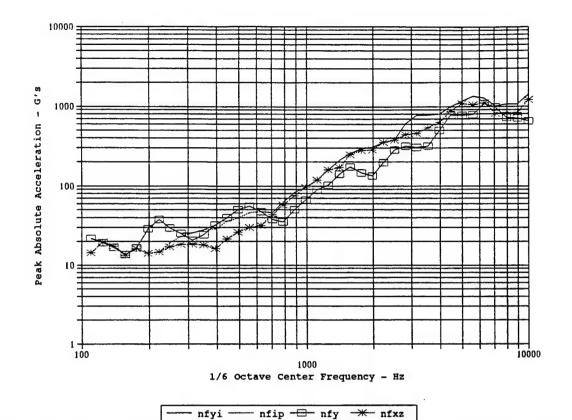


Figure 7(c). G&H 3/8", with Masses, 7000 lb., Various Axis Groupings, SRS (Q=10), Maximum Measured Levels.

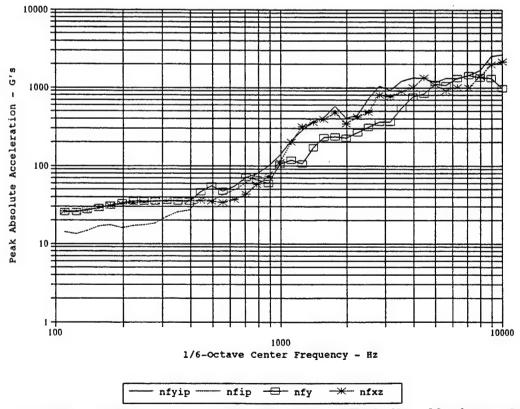


Figure 7(d). HiS 8 mm, with Masses, 2700 lb., Various Axis Groupings, SRS (Q=10), Maximum Measured Levels.

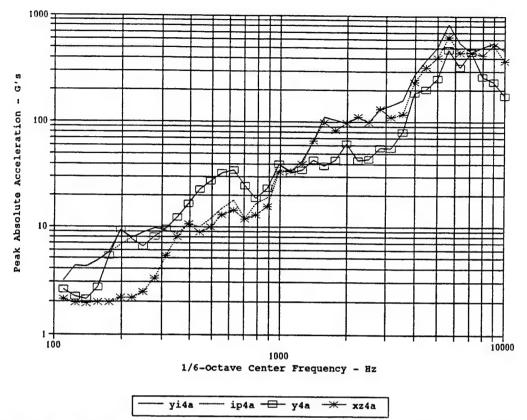


Figure 7(e). LM 3/8", with Masses, Combined 4000 & 4200 lb., Various Axis Groupings, SRS (Q=10), Maximum Measured Levels.

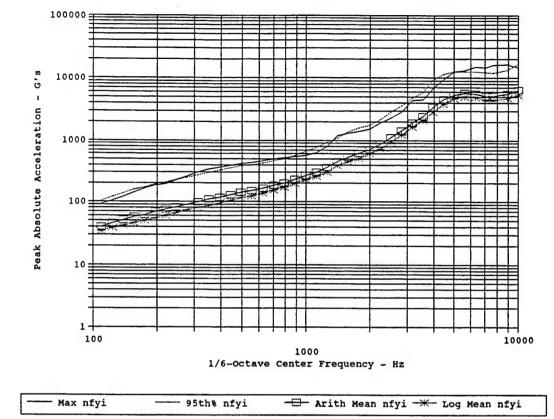


Figure 8(a). OEA 3/8", with Masses, 7000 lb., Combined Normal & In-Plane Resultant, SRS (Q=10), Log-Normal Statistical Features.

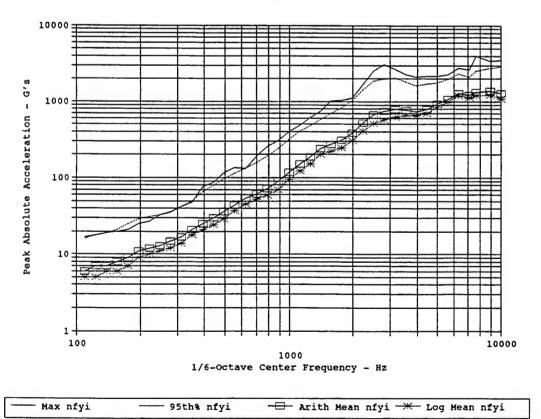


Figure 8(b). HiS 1/2", with Masses, 7000 lb., Combined Normal & In-Plane Resultant, SRS (Q=10), Log-Normal Statistical Features.

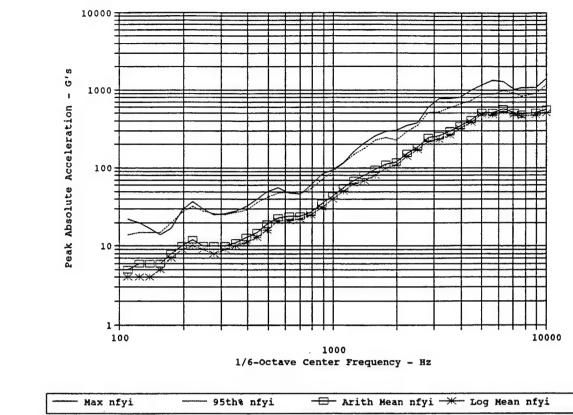


Figure 8(c). G&H 3/8", with Masses, 7000 lb., Combined Normal & In-Plane Resultant, SRS (Q=10), Log-Normal Statistical Features.

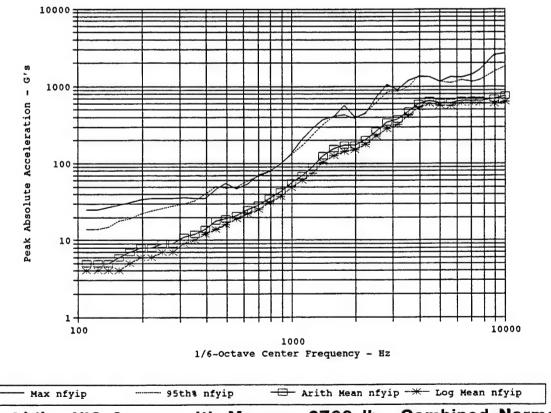


Figure 8(d). HiS 8 mm, with Masses, 2700 lb., Combined Normal & In-Plane Resultant, SRS (Q=10), Log-Normal Statistical Features.

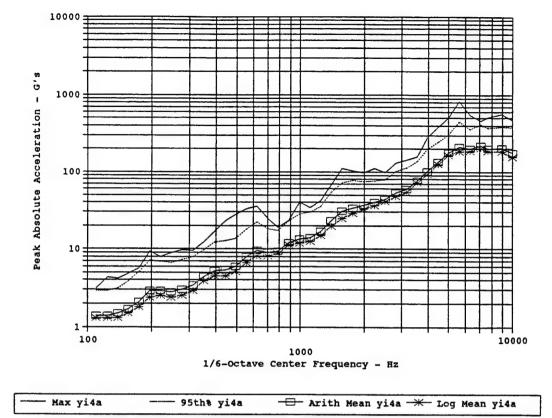


Figure 8(e). LM 3/8", with Masses, Combined 4000 & 4200 lb., Combined Normal & In-Plane Resultant, SRS (Q=10), Log-Normal Statistical Features.

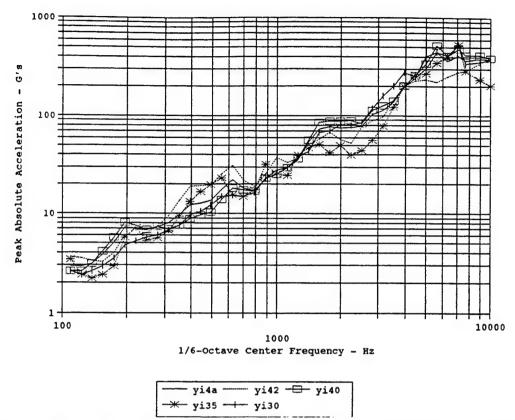


Figure 9(a). LM 3/8", with Masses, Preload Comparison, Combined Normal & In-Plane Resultant, SRS (Q=10), 95th Percentile Levels.

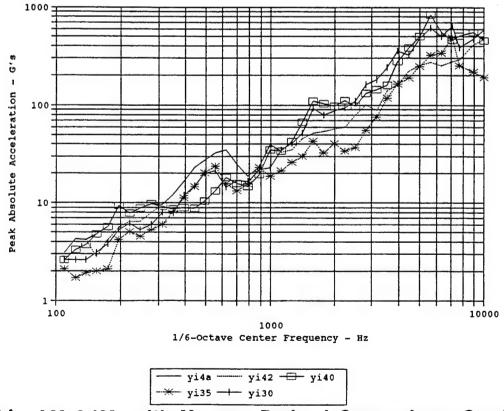


Figure 9(b). LM 3/8", with Masses, Preload Comparison, Combined Normal & In-Plane Resultant, SRS (Q=10), Maximum Measured Levels.

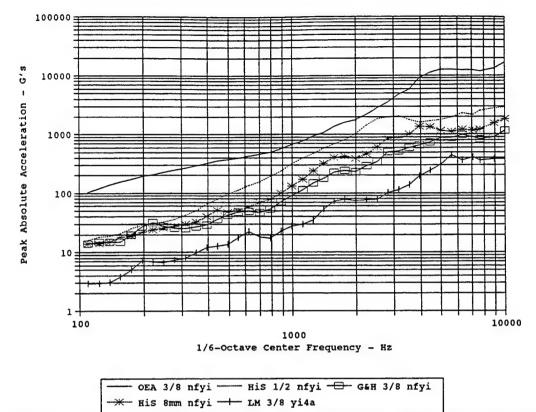


Figure 10(a). Device Comparison, with Masses, Combined Normal & In-Plane Resultant, SRS (Q=10), 95th Percentile Levels.

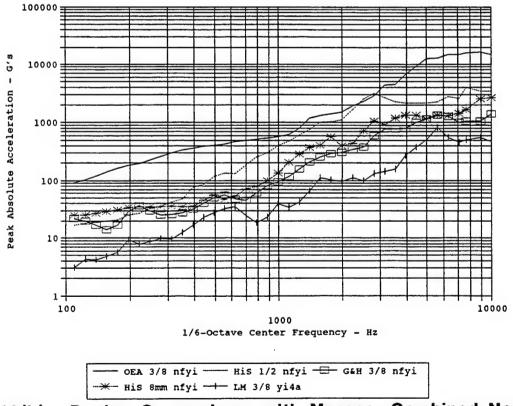


Figure 10(b). Device Comparison, with Masses, Combined Normal & In-Plane Resultant, SRS (Q=10), Maximum Measured Levels.

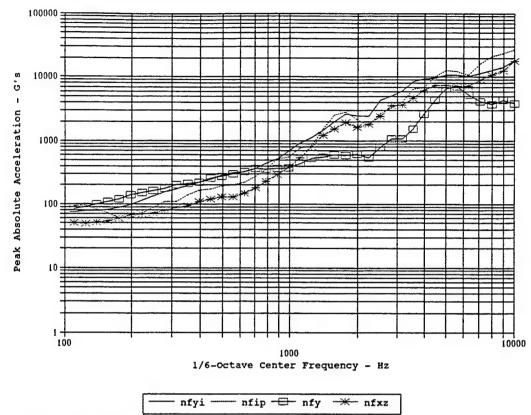


Figure 11(a). OEA 3/8", Bare Panel, 7000 lb., Various Axis Groupings, SRS (Q=10), 95th Percentile Levels.

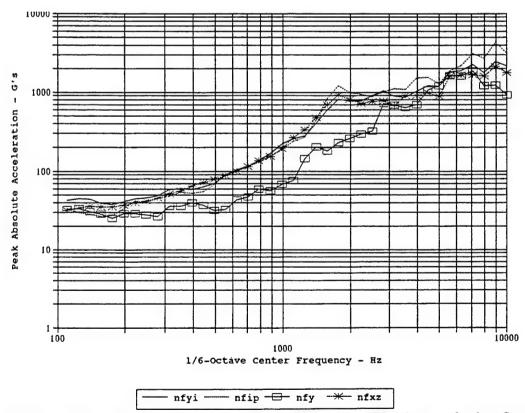


Figure 11(b). HiS 1/2", Bare Panel, 7000 lb., Various Axis Groupings, SRS (Q=10), 95th Percentile Levels.

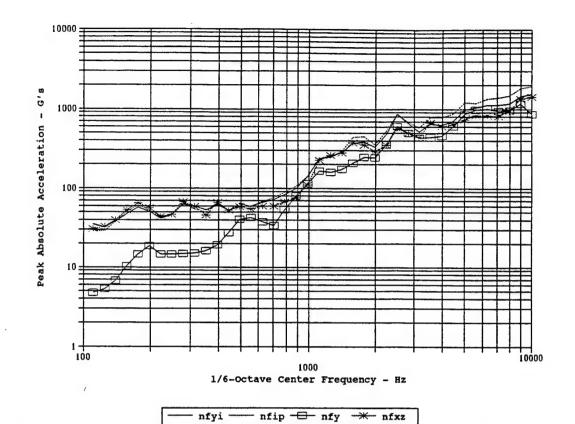


Figure 11(c). G&H 3/8", Bare Panel, 7000 lb., Various Axis Groupings, SRS (Q=10), 95th Percentile Levels.

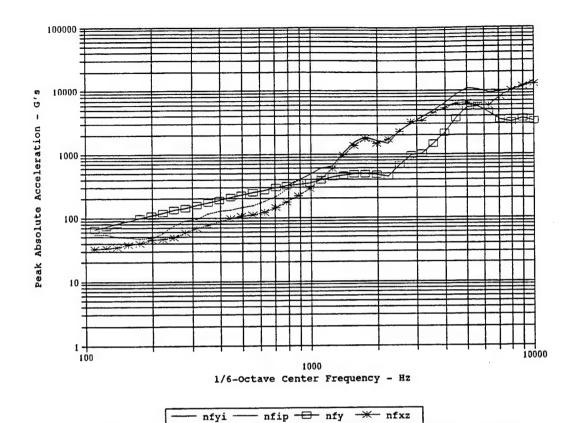


Figure 12(a). OEA 3/8", Bare Panel, 7000 lb., Various Axis Groupings, SRS (Q=10), Maximum Measured Levels.

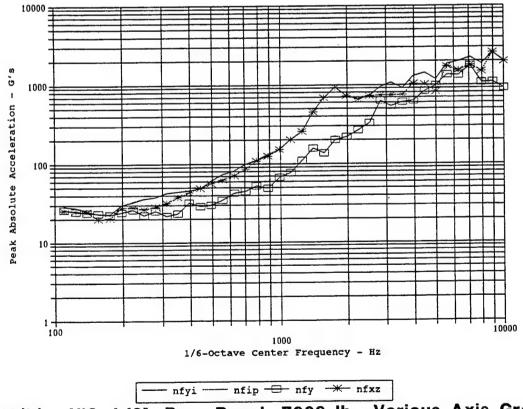


Figure 12(b). HiS 1/2", Bare Panel, 7000 lb., Various Axis Groupings, SRS (Q=10), Maximum Measured Levels.

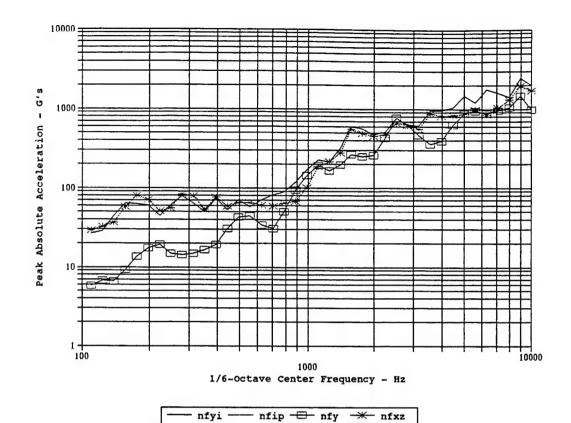


Figure 12(c). G&H 3/8", Bare Panel, 7000 lb., Various Axis Groupings, SRS (Q=10), Maximum Measured Levels.

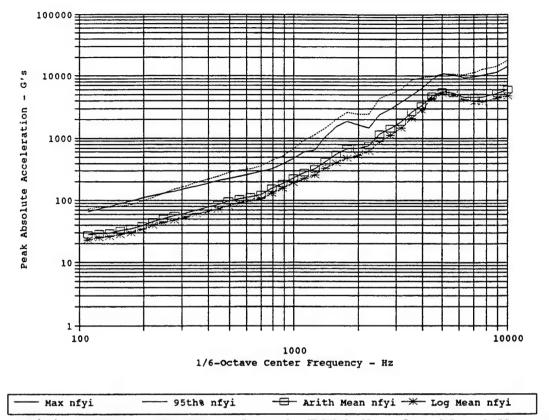


Figure 13(a). OEA 3/8", Bare Panel, 7000 lb., Combined Normal & In-Plane Resultant, SRS (Q=10), Log-Normal Statistical Features.

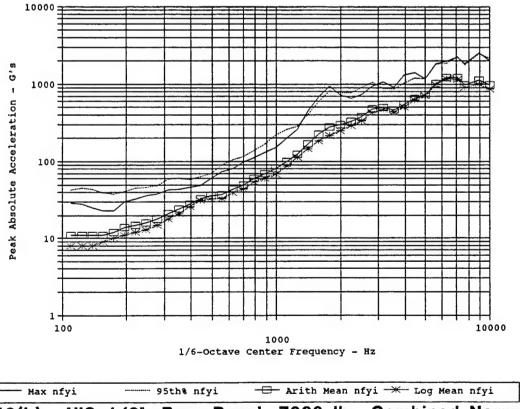


Figure 13(b). HiS 1/2", Bare Panel, 7000 lb., Combined Normal & In-Plane Resultant, SRS (Q=10), Log-Normal Statistical Features.

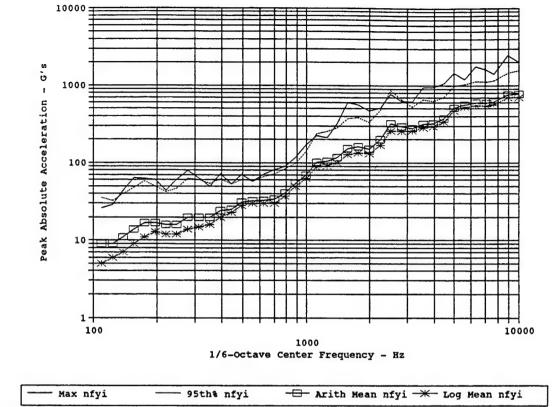


Figure 13(c). G&H 3/8", Bare Panel, 7000 lb., Combined Normal & In-Plane Resultant, SRS (Q=10), Log-Normal Statistical Features.

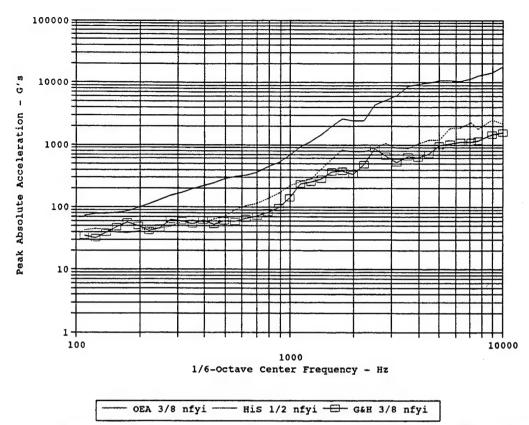


Figure 14(a). Device Comparison, Bare Panel, 7000 lb., Combined Normal & In-Plane Resultant, SRS (Q=10), 95th Percentile Levels.

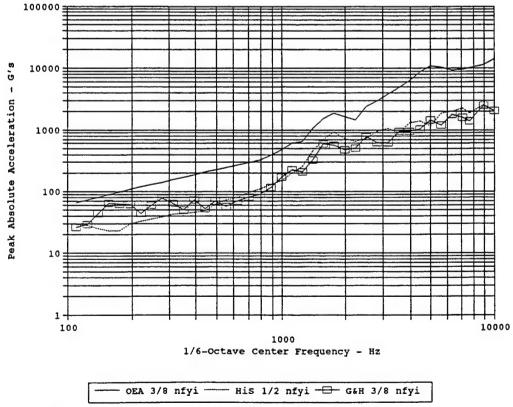


Figure 14(b). Device Comparison, Bare Panel, 7000 lb., Combined Normal & In-Plane Resultant, SRS (Q=10), Maximum Measured Levels.

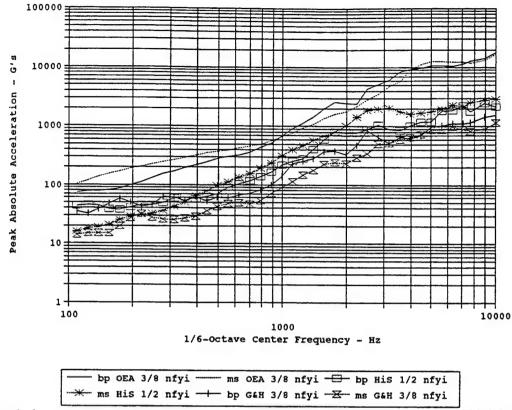


Figure 15(a). Device Comparison, with & without Masses, 7000 lb., Combined Normal & In-Plane Resultant, SRS (Q=10), 95th Percentile Levels.

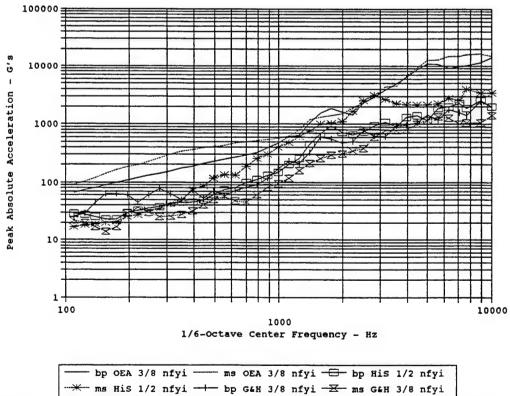


Figure 15(b). Device Comparison, with & without Masses, 7000 lb., Combined Normal & In-Plane Resultant, SRS (Q=10), Maximum Measured Levels.

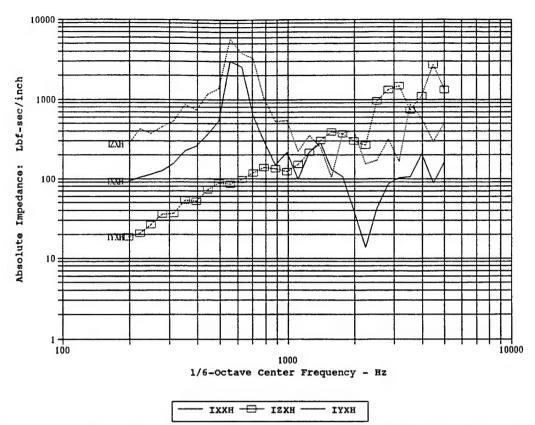


Figure 16. 3/8" Release Device Mounting Point Impedances, X-Direction Tap.

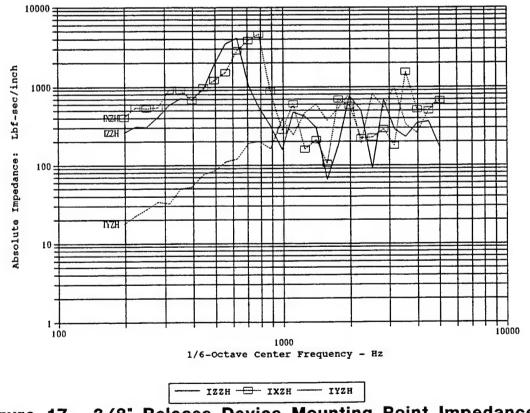


Figure 17. 3/8" Release Device Mounting Point Impedances, Z-Direction Tap.

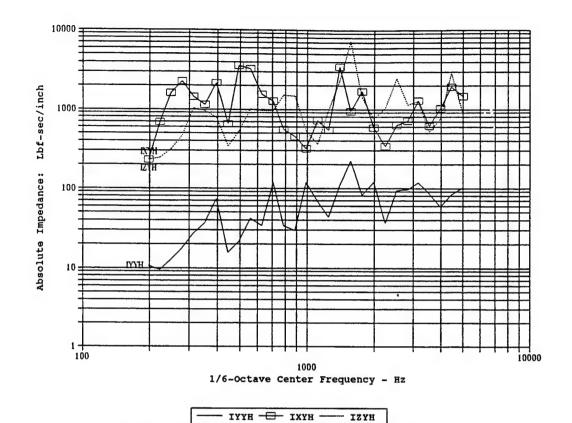


Figure 18. 3/8" Release Device Mounting Point Impedances, Y-Direction Tap.

Mean	Mean	Daviation	Percentile	Maxillium	Boroontilo	Maximum	unce Description	Maximum	ลอเท	Maximum
nfyi	nfyi		nfyi	nfyi	nfip	diju	Aju	υĘν	rercentile	nfxz
40	34	1.861	103	92	26	95	108	88	81	98
46	38	1.915	121	105	113	105	124	98	06	91
	42	1.933	138	121	134	121	135	105	66	97
	46	1.967	156	140	161	140	149	115	109	101
~	20	1.987	172	164	184	164	161	128	119	114
6	55	2.011	193	184	203	184	173	140	129	124
22	9	1.996	208	195	220	195	184	155	135	134
2	99	1.996	227	225	245	225	199	172	141	143
0	73	1.973	247	260	265	260	209	186	151	148
66	80	1.965	268	299	307	299	226	205	166	163
99	87	1.992	298	339	355	339	251	226	178	181
119	95	1.997	327	365	402	365	279	250	189	189
130	104	1.980	354	391	428	391	305	272	202	193
141	115	1.940	375	411	418	411	342	295	220	225
51	124	1.907	393	430	428	430	351	328	237	220
65	137	1.892	427	468	460	468	374	365	252	251
84	154	1.851	464	500	492	200	396	395	282	259
04	174	1.801	497	522	529	522	409	428	324	298
30	196	1.816	571	545	295	545	438	475	389	340
64	226	1.833	668	571	591	571	477	513	514	431
40	258	1.850	922	629	720	629	463	533	692	572
63	304	1.871	931	786	926	786	446	542	868	732
451	384	1.778	1075	1198	1253	1198	474	265	1012	921
33	442	1.880	1367	1293	1457	1293	552	643	1123	1004
4	510	1.895	1601	1392	1593	1392	685	889	1286	1164
14	605	1.816	1760	1507	1708	1507	899	715	1479	1403
69	729	1.851	2195	1917	2028	1917	788	733	1763	1669
1101	925	1.870	2836	2292	2496	2292	1278	1472	2252	2331
1423	1205	1.834	3566	2831	3215	2831	1702	2501	2885	3306
912	1615	1.837	4794	4320	4392	4320	2052	2621	3679	4314
419	2075	1.781	5830	4454	5404	4454	2319	2464	5046	5283
3429	2845	1.912	9026	6705	7929	6705	3624	3462	6614	6397
4534	3848	1.831	11360	9302	10550	9302	5208	4444	8321	7862
5365	4629	1.750	12601	12659	14386	12659	6598	6330	8822	6777
5670	4944	1.692	12663	13062	14121	13062	6330	2503	8731	7844
5614	4899	1.685	12463	14858	14501	14858	5986	6793	8999	8724
5161	4369	1.780	12253	14822	15646	14822	6148	5742	9316	10744
5148	4385	1.748	11905	16178	15537	16178	6129	7231	0296	12043
5654	4818	1.765	13314	16467	15678	16467	5553	7110	10583	12300
147	5003	000	16600	7017		, , ,				

Table A-1(a): OEA 3/8", with Masses, 7000 lb., SRS (Q=10), Log-Normal Statistical Features of Combined Normal & In-Plane, & Various Axis Groupings. Number of Samples = 31 Gumbel Factor = 0.9194

Freq Hz	Arithmetic	Log	Standard	95th Percentile	Maximum	95th Percentile	Maximum	95th Percentile	Maximum	95th	Maximum
	nfyi	nfyi		nfyi	nfyi	nfip	ufip	ufy .	uţ	nfxz	zxJu
110	9	2	1.946	16	17	23	17	10	11	6	14
124	7	5	1.958	18	18	24	18	10	12	10	15
139	7	9	1.955	19	19	24	19	10	12	10	12
156	8	9	2.016	21	20	26	20	12	12	11	12
175	6	7	1.998	25	21	28	21	15	14	12	15
197	11	6	1.977	29	25	30	25	21	20	13	16
221	12	10	1.866	31	27	33	27	22	24	14	. 12
248	13	11	1.820	33	33	34	33	20	17	17	16
278	15	12	1.837	36	35	33	35	23	19	19	17
313	17	14	1.833	42	42	38	42	29	28	23	23
351	21	18	1.809	50	48	46	45	40	48	29	33
394	25	21	1.911	99	92	09	25	25	94	35	37
442	30	24	1.981	79	86	22	89	63	98	43	44
496	36	29	1.989	96	116	92	79	74	116	53	55
222	44	37	1.899	113	135	106	90	94	135	69	69
625	54	45	1.858	134	131	132	131	106	123	98	93
702	62	52	1.878	156	190	167	190	104	103	139	118
787	73	59	1.958	192	253	228	253	104	26	201	176
884	89	20	2.016	239	305	321	305	111	123	290	235
992	118	94	1.997	315	400	410	400	149	153	436	358
1114	152	121	1.986	403	485	548	485	175	176	260	526
1250	188	151	1.932	478	608	711	809	213	215	269	668
1403	243	202	1.831	585	750	805	750	343	321	768	794
1575	274	221	1.919	693	1017	938	1020	306	291	786	780
1768	310	246	1.986	818	1026	1010	1030	271	569	797	773
1984	385	306	2.009	1040	1109	1160	1110	360	352	868	916
2227	521	407	2.048	1429	1667	1560	1670	443	464	1020	1270
2500	672	512	2.088	1861	2510	2360	2510	572	507	1310	1740
2806	749	570	2.029	1972	3104	2910	3100	511	478	1790	2400
3150	795	629	1.952	2032	2682	3120	2680	705	203	1930	2420
3536	777	658	1.768	1786	2274	2560	2270	926	1100	1520	1900
3969	740	643	1.699	1630	2127	2130	2130	1010	993	1220	1500
4454	790	969	1.666	1703	2136	2060	2140	1150	1110	1290	1610
2000	923	842	1.526	1767	2164	2070	2160	1570	1740	1360	1440
5612	1076	1002	1.470	1969	2265	2290	2270	1800	1680	1430	1790
6300	1271	1186	1.459	2300	2778	2870	2780	1810	1550	1730	1810
7071	1211	1129	1.439	2129	2607	2790	2610	1520	1760	1760	1950
7637	1325	1187	1.547	2552	3992	3820	3990	1390	1350	2100	3520
8909		1213	1.602	2773	3433	3840	3430	1370	1480	2210	2760
10000	1277	1094	1.739	2888	3469	3480	3470	1070	1040	2450	3450

Table A-1(b): HiS 1/2", with Masses, 7000 lb., SRS (Q=10), Log-Normal Statistical Features of Combined Normal & In-Plane, & Various Axis Groupings. Number of Samples = 45 Gumbel Factor = 0.9381

Maximum	ofv2	11172	20	47	- 6	2 4	2	<u> </u>	15	17	18	18	18	16	22	26	30	32	43	58	74	95	118	161	170	249	281	284	351	379	440	457	532	623	880	1092	1046	1103	817	838	835	1198
95th	Percentile ofv?	11172	=   =	-			-   \$	7	13	12	12	12	13	15	21	26	33	33	39	48	64	93	144	170	190	255	268	238	314	338	462	442	523	260	688	825	753	757	797	737	792	918
Maximum	ý	AIII.	70	61	14	17	000	63	37	30	25	21	24	32	40	20	56	48	38	35	50	29	89	103	141	174	147	133	196	283	318	306	314	496	692	782	782	1076	975	718	710	649
95th	Percentile	Ž,	+	2 5	+ v	25	2 5	+	53	38	30	56	25	27	33	40	20	48	38	41	57	75	101	138	155	142	148	158	194	264	321	287	309	524	572	665	784	396	892	669	718	555
Maximum	nfin	2	200	17	- 6	16	2	* '	15	19	23	26	28	29	36	39	46	47	46	61	83	95	118	161	210	258	294	306	351	379	602	276	774	798	866	1155	1327	1274	1006	1061	1068	1407
95th	refcentile	2 4	9	9	14	15	ñ	2 4	16	21	22	25	28	31	37	43	49	50	54	99	89	110	129	167	214	285	337	301	365	419	999	989	747	783	921	1151	1047	1074	984	1026	1007	1407
Maximum	iv	200	200	12	14	17	20	67	3/	30	25	26	28	32	40	50	56	48	46	61	83	95	118	161	210	258	294	306	351	379	602	922	774	798	966	1155	1327	1274	1006	1061	1068	1407
95th	reicenine	À	7	2 4	5 5	20	22	17	32	28	26	25	27	29	36	42	48	49	47	54	71	90	115	149	179	229	245	230	296	351	511	517	596	662	732	880	878	981	904	833	868	1168
Standard	Deviation	2000	2.072	2002	1 853	1 882	1 907	100.	1.995	1.972	1.926	1.867	1.794	4.757	1.793	1.703	1.619	1.601	1.542	1,563	1.597	1.591	1.595	1.639	1.722	1.802	1.689	1.520	1.526	1.512	1.636	1.582	1.583	1.514	1.441	1.410	1.416	1.415	1.427	1.401	1.432	1.623
Log	neall		4		2	7	. 0	, ;	2	6	8	6	10	#	13	16	21	21	22	25	31	40	51	63	69	81	98	110	141	170	216	231	566	320	386	482	477	533	484	461	478	200
Arithmetic	nean	. 2	9	9	9	æ	100	2 5	75	10	10	10	11	13	15	19	23	24	24	27	35	44	56	70	80	97	112	120	154	185	244	258	297	348	414	513	509	568	515	488	510	564
Freq Lt.	7	110	124	130	156	175	197	2 6	177	248	278	313	351	394	442	496	222	625	702	787	884	992	1114	1250	1403	1575	1768	1984	2227	2500	2806	3150	3536	3969	4454	2000	5612	6300	7071	7637	8909	10000

Table A-1(c): G&H 3/8", with Masses, 7000 lb., SRS (Q=10), Log-Normal Statistical Features of Combined Normal & In-Plane, & Various Axis Groupings. Number of Samples = 45 Gumbel Factor = 0.9381

Maximum	ubx2	26	26	27	53	30	32	34	34	35	35	36	36	36	35	34	37	44	57	74	110	201	318	358	390	475	345	416	483	798	758	889	1002	1331	1077	908	1016	266	1374	1956	2157
95th	nfxz	9	9	9	9	=	12	13	14	15	16	18	22	26	28	32	40	51	68	94	139	218	300	362	432	452	376	401	510	707	791	915	1056	1143	956	862	837	807	984	1290	1628
Maximum	J.	25	25	27	53	31	34	35	35	35	36	35	35	46	55	47	54	71	29	09	105	118	107	170	230	234	228	566	308	365	367	545	756	829	1110	1057	1302	1432	1327	1318	296
95th Percentile	AJU .	15	15	15	17	18	21	20	19	20	23	25	40	22	49	52	59	63	62	29	84	105	140	212	281	274	566	283	339	408	406	517	781	882	1063	1036	1072	1070	1118	1229	930
Maximum	ajju	14	13	14	17	17	16	17,	17	18	22	56	27	39	35	42	49	61	79	66	136	509	286	373	409	571	402	442	720	1053	917	1202	1328	1324	1156	1322	1291	1436	1653	2520	2649
95th Percentile	diju	=	12	12	14	16	18	20	22	22	24	56	30	35	36	41	48	09	22	111	144	189	301	434	206	531	421	532	775	1216	1122	1130	1343	1440	1284	1290	1409	1321	1408	2032	2527
Maximum	nfvi	25	25	27	59	31	34	35	35	35	36	35	35	46	55	47	54	71	79	66	136	209	286	373	409	571	402	442	720	1053	917	1202	1328	1324	1156	1322	1302	1436	1653	2520	2649
95th Percentile	nfyi	14	4	15	18	19	22	24	26	28	30	33	40	51	48	50	59	69	78	100	131	170	237	321	415	428	387	463	809	850	864	966	1358	1327	1151	1118	1206	1152	1210	1544	1809
Standard		2.152	2.097	2.097	2.234	2.165	2.121	2.171	2.146	2.127	2.053	1.977	2.027	2.070	1.890	1.756	1.753	1.767	1.709	1.760	1.758	1.812	1.918	1.896	1.961	1.861	1.701	1.727	1.744	1.877	1.758	1.630	1.706	1.567	1.491	1.478	1.465	1.434	1.478	1.710	1.816
Log	nfyi	4	4	4	4	5	9	9	7	7	6	10	12	14	16	19	22	25	31	37	49	09	75	104	127	144	152	177	529	281	321	423	531	603	570	563	616	611	609	601	634
Arithmetic Mean	iţ	5	5	5	9	7	8	8	6	6	11	12	14	18	19	21	25	29	35	43	56	70	95	127	157	175	173	204	266	344	376	476	604	662	616	809	664	655	629	869	763
Freq	!	110	124	139	156	175	197	221	248	278	313	351	394	442	496	557	625	702	787	884	992	1114	1250	1403	1575	1768	1984	2227	2500	5806	3150	3536	3969	4454	2000	5612	9300	7071	7637	8909	10000

Table A-1(d): HiS 8 mm, with Masses, 2700 lb., SRS (Q=10), Log-Normal Statistical Features of Combined Normal & In-Plane, & Various Axis Groupings. Number of Samples = 43 Gumbel Factor = 0.9360

Maximum	x74a	2	2	2	2	2	2	2	2	3	5	8	=	6	10	13	14	12	13	16	33	34	40	29	66	83	98	112	66	132	110	117	235	326	404	635	453	458	428	529	372
	rercentile xz4a	Dr. C	2	2	2	2	2	2	2	2	က	4	9	9	7	13	15	=	=	15	26	38	40	51	70	72	7.1	89	87	112	106	124	167	218	266	405	362	396	384	375	313
Maximum	v4a	33	2	2	3	2	6	8	9	8	10	12	17	23	28	33	35	25	19	23	40	33	35	44	38	44	62	43	44	22	99	80	187	202	257	482	328	459	268	235	174
95th	rercentile v4a	33	2	2	ဗ	2	10	6	7	8	8	11	15	15	17	23	29	23	19	52	29	24	28	39	36	45	20	44	46	26	54	85	144	189	264	386	297	383	255	226	169
Maximum	io4a	3	4	4	5	9	7	8	6	10	6	6	F	10	12	15	18	12	17	19	35	34	42	29	111	104	98	112	66	132	144	158	278	386	505	836	553	458	508	558	468
95th	rercenule io4a	3	3	4	4	5	5	5	7	7	7	6	10	10	11	12	15	13	16	21	29	38	45	20	113	105	66	106	105	139	150	159	212	307	376	574	435	469	505	529	472
Maximum	vi4a	3.1	4.3	4.2	4.8	5.7	9.3	7.9	8.8	9.7	9.6	12.3	16.8	23	27.6	32.6	35	24.7	18.7	23.4	39.7	33.9	42.4	29	110.7	103.8	98.1	111.9	98.8	131.6	143.6	158.3	277.5	385.9	504.6	835.6	552.9	458.8	508.5	558.4	467.6
95th	vi4a	2.9	2.9	3.1	3.8	5.1	7.2	6.9	6.7	7.3	8	9.7	12.2	12.8	13.6	17.8	22.2	18.1	17.1	23.1	27.8	29.6	35.5	54.1	72.9	77.5	75.3	76.4	78.6	102.6	113.1	138.5	196.5	244.1	307.1	448.8	360.2	413.7	368.2	383.2	378.9
Standard	Deviation	1.580	1.589	1.642	1.697	1.802	1.880	1.807	1.795	1.826	1.791	1.679	1.755	1.819	1.745	1.741	1.772	1.584	1.469	1.523	1.632	1.647	1.638	1.783	1.850	1.777	1.621	1.533	1.455	1.537	1.524	1.455	1.523	1.460	1.424	1.664	1.453	1.496	1.477	1.512	1.652
Log	viđa Viđa	13	1.3	1.3	1.5	1.8	2.4	2.5	2.4	2.5	2.9	3.9	4.5	4.5	5.1	6.7	8.1	8.1	8.7	11.1	11.8	12.4	14.9	19.6	24.8	28.3	32.3	36.1	40.7	48.3	54	71.8	93.9	125.7	165.2	183.8	187	204	185.9	185.6	157.2
Arithmetic	vi4a	4.1	4.1	1.5	1.7	2.1	2.9	2.9	2.8	3	3.4	4.4	5.3	5.4	9	7.9	9.6	6	9.4	12	13.3	41	16.8	23.1	30.4	33.4	36.5	39.9	43.8	53.3	59.4	77	102.6	135.5	176.8	212.5	201.4	221.7	201.6	203.4	179.1
Freq	7	110	124	139	156	175	197	221	248	278	313	351	394	442	496	257	625	702	787	884	992	1114	1250	1403	1575	1768	1984	2227	2500	2806	3150	3536	3969	4454	2000	5612	6300	7071	7637	8909	10000

Table A-1(e): LM 3/8", with Masses, Combined 4000 & 4200 lb., SRS (Q=10), Log-Normal Statistical Features of Combined Normal & In-Plane, & Various Axis Groupings. Number of Samples = 45 Gumbel Factor = 0.9381

Freq Hz	Arithmetic	Log	Standard	95th	
1 147 1			Standard		Maximum
''2	Mean	Mean	Deviation	Percentile	
	yi42	yi42		yi42	yi42
110	1.6	1.5	1.592	3.6	3.1
124	1.6	1.5	1.586	3.5	4.3
139	1.6	1.5	1.527	3.3	4.2
156	1.8	1.7	1.369	3.2	2.8
175	2.1	2	1.441	4	4.2
197	2.8	2.6	1.557	6	5.6
221	3.1	2.9	1.484	6	6.5
248	3.2	2.9	1.500	6.3	6.5
278	3.4	3.1	1.583	7.4	8
313	4.4	4	1.576	9.5	9.6
351	6	5.3	1.644	13.7	12.3
394	7.6	6.6	1.748	19	16.8
442	7.7	6.5	1.767	19.2	23
496	8.5	7.3	1.680	19.6	27.6
557	11	9.5	1.689	25.6	32.6
625	12.9	10.9	1.736	31	35
702	10	8.9	1.610	21.8	24.7
787	9.1	8.2	1.562	19	18.7
884	11.3	10.1	1.633	25.6	23.4
992	15.3	13.3	1.728	37.5	39.7
1114	15.4	13.9	1.587	33.3	32.9
1250	17.9	16.3	1.548	37.2	34.8
1403	25	22.9	1.525	51	45.7
1575	27.4	25.1	1.545	57.2	52.2
1768	31.5	28.7	1.577	68	54
1984	30.7	28.9	1.438	57.5	57.2
2227	31.1	29.7	1.352	52.6	60.2
2500	42.7	40.3	1.409	77.2	79.3
2806	50.8	48.2	1.383	89	101.8
3150	52.5	49.3	1.432	97.4	89.3
3536	75.5	70.6	1.468	145.9	140.3
3969	93.3	85.4	1.565	199.4	160.6
4454	118.8	111.1	1.458	227	220.3
5000	141.9	136.5	1.326	232.8	253.9
5612	130.4	123.9	1.358	221	271.6
6300	157.1	152	1.301	250	250.5
7071	172.8	166.6	1.322	282.5	278.1
7637	167.4	159.7	1.358	285	290.9
8909	180.3	166.4	1.480	349.4	410.3
10000	162.3	138.6	1.739	395	467.6

Table A-1(f): LM 3/8", with Masses, 4200 lb., SRS (Q=10), Log-Normal Statistical Features of Combined Normal & In-Plane, & Various Axis Groupings. Number of Samples = 15 Gumbel Factor = 0.8688

Freq	Arithmetic	Log	Standard	95th	Maximum
Hz	Mean	Mean	Deviation	Percentile	
	yi40	yi40	Dovidion	yi40	yi40
110	1.3	1.2	1.555	2.6	2.6
124	1.3	1.2	1.570	2.6	3.3
139	1.4	1.2	1.686	3.1	3.7
156	1.7	1.4	1.823	4.1	4.8
175	2.1	1.7	1.959	5.7	5.7
197	2.9	2.3	2.034	8.1	9.3
221	2.8	2.3	1.939	7.5	7.9
248	2.6	2.2	1.896	6.8	8.8
278	2.8	2.3	1.909	7.3	9.7
313	2.9	2.5	1.781	6.9	9.2
351	3.7	3.3	1.586	7.6	8.7
394	4.2	3.8	1.601	8.8	9
442	4.2	3.7	1.694	9.6	8.8
496	4.8	4.3	1.635	10.3	10.5
557	6.3	5.7	1.638	13.8	13.3
625	8	7	1.701	18.2	18.3
702	8.5	7.8	1.573	17.5	15.7
787	9.6	9	1.425	17	14.8
884	12.3	11.6	1.466	23	19.6
992	12.2	11.1	1.577	25.1	35
1114	13.3	11.6	1.672	29.3	33.9
1250	16.3	14.3	1.684	36.4	42.4
1403	22.1	18.2	1.886	56.7	67
1575	31.9	24.7	2.003	85.7	110.7
1768	34.3	28	1.884	87.3	103.8
1984	39.3	34.2	1.698	88.3	98.1
2227	44.3	39.8	1.570	89.4	111.9
2500	44.4	40.9	1.486	83.3	98.8
2806	54.6	48.3	1.615	114.1	131.6
3150	62.9	56.5	1.566	126.2	143.6
3536	77.7	72.4	1.457	142.2	158.3
3969	107.3	98.5	1.501	204	277.5
4454	143.9	133.7	1.448	259.5	385.9
5000	194.3	181.8	1.420	340.8	504.6
5612	253.5	224	1.610	526.1	835.6
6300	223.5	207.4	1.464	410.9	552.9
7071	246.2	225.8	1.523	480.1	458.8
7637	218.6	200.6	1.505	417.6	508.5
8909	215	196.1	1.521	415.8	558.4
10000	187.5	167.4	1.602	389.5	455.4

Table A-1(g): LM 3/8", with Masses, 4000 lb., SRS (Q=10), Log-Normal Statistical Features of Combined Normal & In-Plane, & Various Axis Groupings. Number of Samples = 30 Gumbel Factor = 0.9175

Freq	Arithmetic	Log	Standard	95th	Maximum
Hz	Mean	Mean	Deviation	Percentile	
	yi35	yi35		yi35	yi35
110	1.3	1.2	1.654	3.4	2.1
124	1.2	1.1	1.465	2.4	1.7
139	1.1	1	1.438	2.2	1.9 、
156	1.3	1.2	1.400	2.4	2
175	1.5	1.4	1.418	2.9	2.1
197	2.4	2.1	1.618	5.7	4.2
221	2.8	2.5	1.667	7.1	5.1
248	2.3	2.1	1.590	5.3	4.5
278	2.6	2.4	1.516	5.6	5.3
313	3.1	2.9	1.498	6.6	6
351	4.3	4	1.522	9.4	8.2
394	5.6	5	1.608	13.3	11.2
442	5.7	4.8	1.841	16.6	14.8
496	7	5.9	1.817	19.8	20.3
557	8.6	7.2	1.775	23.3	23.7
625	6.8	6.2	1.572	15.5	15.7
702	7.2	6.7	1.480	14.9	13.4
787	10.7	10.4	1.288	17.4	15.6
884	16.5	15.7	1.421	32.1	23.1
992	21.1	11.4	1.486	25.5	18.6
1114	11.4	10.5	1.509	24.4	21.4
1250	16.7	15.2	1.594	39.4	25.8
1403	17.9	16	1.701	47.3	29.9
1575	21.1	19	1.631	51.4	42.9
1768	22.5	21.5	1.384	41.8	32.5
1984	24.3	22.8	1.464	49.7	40.6
2227	24.2	23.6	1.287	39.5	34
2500	28.1	27.4	1.266	44.4	37.2
2806	37.6	36.9	1.230	56.2	55.6
3150	43.8	42	1.355	77.9	76.3
3536	63.7	60.2	1.415	122	118.1
3969	107.5	102.7	1.39	200.9	163.1
4454	150.5	145.1	1.349	266.9	187.6
5000	192.4	190	1.183	267.5	248
5612	206.4	199.7	1.313	347.5	323
6300	230.7	222.5	1.333	399.8	338.7
7071	259.6	242.6	1.467	529.8	485.3
7637	167.7	162.1	1.323	286.8	250.8
8909	153.9	150.9	1.235	232.2	218.3
10000	131.6	128.8	1.247	202	192.8

Table A-1(h): LM 3/8", with Masses, 3500 lb., SRS (Q=10), Log-Normal Statistical Features of Combined Normal & In-Plane, & Various Axis Groupings. Number of Samples = 15 Gumbel Factor = 0.8688

Freq	Arithmetic	Log	Standard	95th	Maximum
Hz	Mean	Mean	Deviation	Percentile	
	yi30	yi30		yi30	yi30
110	1.2	1.1	1.610	2.6	2.6
124	1.2	1.1	1.565	2.4	2.6
139	1.2	1.1	1.661	2.6	2.6
156	1.3	1.2	1.676	2.9	3.1
175	1.6	1.5	1.648	3.5	3.8
197	2.1	1.9	1.695	4.7	5.3
221	2.3	2	1.712	5.2	6.2
248	2.4	2.1	1.775	5.7	5.3
278	2.5	2.1	1.802	6	6
313	2.9	2.5	1.758	6.7	8
351	3.6	3.2	1.631	7.6	7.9
394	4.4	3.8	1.696	9.6	11.8
442	4.5	3.9	1.764	10.4	14.9
496	5.2	4.5	1.770	12.2	20.1
557	6.7	5.8	1.720	15	21.3
625	7.1	6.4	1.651	15.3	14.4
702	7.6	6.9	1.549	14.9	16.9
787	9	8.4	1.465	16.5	16.5
884	12.3	11.4	1.485	22.9	21.9
992	12.7	11.6	1.566	25.4	22.8
1114	13.6	11.9	1.680	29.6	35
1250	17.4	15.2	1.706	38.8	41.1
1403	19.5	16.9	1.705	43.1	51.7
1575	27.8	22.6	1.866	67.4	92.5
1768	30.7	26.2	1.747	69.7	79.6
1984	38.4	34.4	1.623	80.5	87.2
2227	38.3	34.1	1.621	79.5	94.7
2500	42.2	37.9	1.586	85	109.4
2806	55.7	49.1	1.649	118	160.5
3150	74.8	66	1.648	158.5	181.2
3536	100.5	90.7	1.573	200.6	241.8
3969	133.8	119.1	1.623	278.3	359.5
4454	140.3	130.7	1.45	250.7	325.5
5000	207.8	188.5	1.545	404.5	482.9
5612	224	200.4	1.581	447.6	616.3
6300	216.8	198.8	1.514	411.7	505
7071	257.3	229.8	1.608	528.6	637.8
7637	183.8	169.5	1.497	344	386.4
8909	193.4	178	1.489	357.7	473
10000	185.6	166.4	1.580	371.4	585.9

Table A-1(i): LM 3/8", with Masses, 3000 lb., SRS (Q=10), Log-Normal Statistical Features of Combined Normal & In-Plane, & Various Axis Groupings. Number of Samples = 45 Gumbel Factor = 0.9381

Freq H2	Arithmetic	Log	Standard	95th Percentile	Maximum	95th	Maximum	95th	Maximum	95th	Maximum
!	nfyi	nfyi		nfyi	nfvi	nfip	dju	Ju	Ju	Ufxz	nfxz
110	28	23	1.810	74	99	94	56	84	99	50	33
124	29	25	1.801	78	74	92	55	91	74	49	33
139	30	56	1.762	79	81	83	50	66	81	52	35
156	33	28	1.734	82	90	72	90	108	06	54	38
175	35	30	1.714	87	66	09	48	119	66	59	40
197	39	34	1.720	66	109	09	48	138	109	68	45
221	46	40	1.710	113	120	72	28	152	120	89	47
248	51	44	1.750	131	132	88	22	162	132	7.1	50
278	57	48	1.807	154	142	109	92	177	142	79	59
313	63	54	1.814	173	157	110	95	203	157	87	69
351	71	61	1.834	199	174	140	117	211	174	94	77
394	79	99	1.854	222	189	166	127	221	189	108	87
442	98	72	1.877	247	210	171	133	256	210	120	97
496	98	82	1.888	284	228	194	146	272	228	129	107
557	107	90	1.883	310	249	204	156	302	249	130	112
625	116	98	1.852	327	271	219	182	330	271	148	123
702	127	107	1.864	362	298	275	217	361	298	181	145
787	156	132	1.861	444	320	349	277	354	320	228	177
884	187	159	1.834	520	391	521	391	365	333	292	219
992	229	191	1.919	685	475	558	475	376	346	378	286
1114	281	226	2.055	923	209	292	209	433	390	542	407
1250	324	258	2.122	1124	650	822	650	533	432	812	596
1403	426	333	2.122	1449	1051	1535	1051	559	464	1221	996
1575	549	406	2.245	1978	1537	2544	1537	009	480	1517	1367
1768	675	486	2.360	2607	1849	2819	1849	588	488	1945	1733
1984	689	527	2.199	2461	1625	2186	1625	620	472	1639	1458
2227	765	618	2.012	2427	1448	1720	1448	547	442	1819	1713
2500	1163	872	2.279	4372	2367	2693	2367	781	680	2436	2276
2806	1432	1103	2.191	5115	2933	3314	2933	1079	959	3565	3214
3150	1837	1450	2.085	6106	3847	4129	3847	1061	1016	3675	3333
3536	2614	2076	2.058	8522	4898	6500	4898	1521	1457	4684	4485
3969	3349	2849	1.833	9327	6319	2003	6319	2647	2144	6270	5268
4454	4727	4379	1.502	9710	8674	10139	8674	4372	3685	7415	6255
2000	5586	5252	1.435	10642	10967	12712	10967	6682	5417	7373	6419
5612	5316	4946	1.484	10713	10591	12242	10591	7152	5744	7290	5800
6300	4589	4157	1.595	10367	9401	10789	9401	5319	4558	7315	5821
7071	4555	3938	1.732	11538	9648	16415	9648	4222	3474	9037	8117
7637	4608	3794	1.871	12924	10210	21477	10210	3744	3230	10699	10157
8303	5242	4357	1.841	14384	11570	23549	11570	4368	3695	12431	11749
10000	5991	4784	1.972	18074	14280	26800	14280	3813	3258	17640	12885

Table A-2(a): OEA 3/8", Bare Panel, 7000 lb., SRS (Q=10), Log-Normal Statistical Features of Combined Normal & In-Plane, & Various Axis Groupings. Number of Samples = 11 Gumbel Factor = 0.8407

Table A-2(b): HiS 1/2", Bare Panel, 7000 lb., SRS (Q=10), Log-Normal Statistical Features of Combined Normal & In-Plane, & Various Axis Groupings. Number of Samples = 15 Gumbel Factor = 0.8688

-			:					:			
HZ H	Mean	Mean	Deviation	Percentile	1.4	Percentile	3	Percentile		Percentile	,
$\dashv$	iÁu	À		ığı	IŊI	ulip	uţib	λ	ΔĮu	ntxz	nfxz
110	6	5	2.929	35	26	53	26	2	9	31	59
124	6	9	2.686	32	29	59	29	5	7	33	32
139	11	7	2.610	39	44	37	44	7	2	40	96
3	14	6	2.566	48	64	90	64	10	6	23	58
175	17	11	2.520	58	63	09	63	15	14	99	80
	17	13	2.166	50	61	54	61	19	17	99	71
221	16	12	2.009	42	44	4	44	15	19	44	51
m	16	12	2.112	46	09	46	09	15	15	47	56
8	20	14	2.330	63	79	65	79	15	14	68	83
3	20	15	2.205	9	64	54	64	15	15	59	79
_	20	16	2.017	54	50	90	50	16	17	46	54
394	24	20	1.927	62	73	64	73	19	19	99	9/
2	25	23	1.613	53	53	52	53	28	31	52	59
9	31	28	1.539	09	71	65	7.1	14	42	59	99
557	32	30	1.480	59	57	58	57	42	44	54	65
625	33	30	1.557	99	71	69	71	38	34	09	61
2	34	30	1.658	72	82	9/	82	34	31	09	58
7	41	37	1.585	83	90	89	06	54	20	29	64
4	54	20	1.476	66	117	107	117	81	94	92	29
2	20	63	1.581	141	172	141	172	113	143	111	100
1114	102	88	1.744	235	225	238	225	165	193	226	186
1250	106	92	1.792	255	213	248	213	159	165	261	214
1403	118	100	1.816	284	324	295	324	175	195	279	280
'5	155	129	1.822	370	598	445	598	207	265	376	554
98	162	136	1.798	381	562	450	293	247	251	354	489
1984	151	132	1.699	332	471	359	471	242	259	291	452
27	200	167	1.824	481	509	524	609	357	426	354	475
2500	324	260	1.978	861	778	870	772	909	778	569	629
90	292	254	1.725	662	622	684	809	201	622	205	641
3150	280	260	1.483	519	617	581	617	433	467	443	551
96	318	283	1.613	654	949	795	949	441	358	673	874
99	322	292	1.544	625	951	787	951	460	392	603	812
54	372	339	1.521	202	1044	878	1044	604	624	644	826
00	515	472	1,518	286	1451	1209	1451	855	698	739	864
12	558	517	1.488	1038	1200	1190	1200	974	935	837	972
6300	602	554	1.494	1120	1781	1326	1781	1009	874	824	844
1	592	545	1.505	1116	1580	1393	1580	942	953	811	1025
7637	618	568	1.500	1157	1403	1469	1403	961	1051	963	1308
8909	763	969	1.515	1444	2477	1806	2477	1158	1454	1336	1975
1											

Table A-2(c): G&H 3/8", Bare Panel, 7000 lb., SRS (Q=10), Log-Normal Statistical Features of Combined Normal & In-Plane, & Various Axis Groupings. Number of Samples = 44 Gumbel Factor = 0.9370

1/6-Octave	X-Direction	Y-Direction	Z-Direction
Freq	Lbf-Sec/	Lbf-Sec/	Lbf-Sec/
Hz	Inch	Inch	Inch
197	93.1	18.8	273.2
221	105	20.7	425.5
248	113.9	26.7	371.9
278	126.8	35.7	458.8
312	156.9	36.2	539.7
351	225.9	53.4	861.7
394	259.6	52.1	739.7
442	363.4	72.2	1157.6
496	534.8	87.7	1367.9
557	3009.6	84.8	5666.7
625	2570.9	98.1	3770.8
702	626.2	117.9	3254.8
787	302.6	139.1	1044.4
884	148.8	133.9	526.1
992	216.6	123.3	550.1
1114	96.6	150.2	221.6
1250	219.6	214.6	351.9
1402	286.8	303.6	248.8
1574	131.7	389.8	105.4
1767	107.1	370.4	373.7
1984	39.6	299.5	402.3
2227	13.6	264.2	154.9
2500	42.6	961.3	172.1
2806	85.8	1305.8	318
3149	103.4	1460.4	166.4
3535	106.8	734.4	874.7
3968	205.8	1098	574.8
4454	87.9	2718.1	292.3
5000	161.3	1318	505.2

Table A-3(a): "Foot" Impedances for 3/8" Mount, X-Direction Tap.

V 51 11	V D:	7 D'1'
		Z-Direction
		Lbf-Sec/
		Inch
401		260.2
545.5	22.6	312.2
522.4	27.1	306
549.9	33.7	411
913.7	32	588.8
904.9	49.8	710.1
670.9	52.4	694.9
975.3	76.7	916.8
1211.7	84.4	1884.2
1516.7	109.4	3478.1
2856.5	120.2	4143.2
3818.5	190.7	1063.6
4550.9	201.6	545.7
880.6	162.5	315.8
279.8	383.4	157.8
601.2	243.5	470.1
159.4	467.4	417.8
210.2	600.4	298.7
104.1	369	65.3
694.3	524.5	180.1
570.9	819.9	766.9
222.6	189.7	498.1
224.5	815.6	90.9
289.1	543.5	690.4
177.5	1017.5	288.5
1526.2	332.7	229.3
514	260.9	346.5
496.1		
676.1	740.5	169.2
	522.4 549.9 913.7 904.9 670.9 975.3 1211.7 1516.7 2856.5 3818.5 4550.9 880.6 279.8 601.2 159.4 210.2 104.1 694.3 570.9 222.6 224.5 289.1 177.5 1526.2 514 496.1	Lbf-Sec/Inch         Lbf-Sec/Inch           401         17.8           545.5         22.6           522.4         27.1           549.9         33.7           913.7         32           904.9         49.8           670.9         52.4           975.3         76.7           1211.7         84.4           1516.7         109.4           2856.5         120.2           3818.5         190.7           4550.9         201.6           880.6         162.5           279.8         383.4           601.2         243.5           159.4         467.4           210.2         600.4           104.1         369           694.3         524.5           570.9         819.9           222.6         189.7           224.5         815.6           289.1         543.5           177.5         1017.5           1526.2         332.7           514         260.9           496.1         508.9

Table A-3(b): "Foot" Impedances for 3/8" Mount, Z-Direction Tap.

4/0.0=4=+=	V Discotis	V Discotic :	7 Direction
1/6-Octave	X-Direction	Y-Direction	Z-Direction
Freq	Lbf-Sec	Lbf-Sec	Lbf-Sec
Hz	Inch	Inch	Inch
197	230.1	10.6	231.6
221	689.3	9.4	244.9
248	1593.1	12.6	309.7
278	2283.2	17.8	467.7
312	1435	27.1	1021.9
351	1134.5	36.1	964.6
394	2144.7	73	795.4
442	652.1	15.7	339.2
496	3545.2	21.6	525.2
557	3275.5	41.6	1002.7
625	1542.9	34	952.5
702	1278.8	117.6	953.8
787	559.8	33.8	1500.8
884	447.1	29.7	1446.6
992	318.7	117.9	535
1114	719.1	68.9	365.7
1250	549.2	43.1	971.3
1402	3452.3	108.8	2301.2
1574	945	221	7246.7
1767	1691.6	82.2	1409.1
1984	588.4	119.3	749.5
2227	336.3	36.6	1050
2500	630.8	93.9	2467
2806	709.8	95.1	1137.7
3149	1279.8	119	1259.1
3535	613.1	86.5	518.8
3968	1031.4	59	768.2
4454	1931.2	83.2	2908.4
5000	1454	103	876.7

Table A-3(c): "Foot" Impedances for 3/8" Mount, Y-Direction Tap.

## REPORT DOCUMENTATION PAGE

Form Approved OMB No. 0704-0188

Highway, Suite 1204, Arlington, VA 22202–4302, and to the Office of Management and Budget, Paperwork Reduction Project (0704-0188), Washington, DC 20503.					
2. REPORT DATE	3. REPORT TYP	PE AND DATES COVERED			
December 1996	Technical M	Memorandum			
		5. FUNDING NUMBERS			
Comparison of Separation Shock for Explosive and Nonexplosive Release Actuators on a Small Spacecraft Panel		WU 233-10-14-04			
		†			
Woolley					
7. PERFORMING ORGANIZATION NAME(S) AND ADDRESS(ES)					
		REPORT NUMBER			
(S) AND ADDRESS(ES)		10. SPONSORING / MONITORING			
ministration		AGENCY REPORT NUMBER			
		NASA TM-110257			
esearch Center, Hampto	n, Virginia; <b>and</b>	Woolley: Lockheed Martin,			
		12b. DISTRIBUTION CODE			
		•			
37					
Availability: NASA CASI, 301-621-0390					
Shock, safety, overall system costs, and emergence of new technologies have raised concerns regarding continued use of pyrotechnics on spacecraft. NASA Headquarters requested Langley Research Center (LaRC) study pyrotechnic alternatives using nonexplosive actuators (NEAs), and LaRC participated with Lockheed Martin Missile and Space Co. (LMMSC) in objectively evaluating applicability of some NEA mechanisms to reduce small spacecraft and booster separation event shock. Comparative tests were conducted on a structural simulator using five different separation nut mechanisms, three pyrotechnics from OEA Aerospace and Hi-Shear Technology and two NEAs from G & H Technology and LMMSC. Multiple actuations were performed with preloads up to 7,000 pounds, 7,000 being the standard. All devices except the LMMSC NEA rotary nut concept were available units with no added provisions to attenuate shock. Accelerometer measurements were recorded, reviewed, processed into Shock Response Spectra (SRS) and comparisons performed. For the standard preload, pyrotechnics were the most severe and the G & H NEA the least severe. Comparing all results, the LMMSC concept produced the lowest levels with preload limited to ~4,200 pounds. Testing this concept over a range of 3,000 to 4,200 pounds indicated no effect on shock. This report presents data from these tests and the comparative results.					
	2. REPORT DATE December 1996  Explosive and Nonexploatel  Woolley  ADDRESS(ES)  (S) AND ADDRESS(ES)  ministration  esearch Center, Hampto diquarters requested Langle and LaRC participated with Lane NEA mechanisms to reded on a structural simulator Hi-Shear Technology and two sup to 7,000 pounds, 7,000 with no added provisions to ck Response Spectra (SRS the G & H NEA the least se limited to ~4,200 pounds.	2. REPORT DATE December 1996  Explosive and Nonexplosive Release nel  Woolley  ADDRESS(ES)  (S) AND ADDRESS(ES)  ministration  esearch Center, Hampton, Virginia; and december and LaRC participated with Lockheed Martin Me NEA mechanisms to reduce small space and LaRC participated with Lockheed Martin Me NEA mechanisms to reduce small space and LaRC participated with Lockheed Martin Me NEA mechanisms to reduce small space and to a structural simulator using five difference on a structural simulator using five difference is up to 7,000 pounds, 7,000 being the standard with no added provisions to attenuate shock. Ck Response Spectra (SRS) and comparison the G & H NEA the least severe. Comparing limited to ~4,200 pounds. Testing this concept.			

spacecraft design, testing, and performance; spacecraft propulsion and power; 52 mechanical engineering; launch vehicle and space vehicle 16. PRICE CODE A04 20. LIMITATION OF ABSTRACT 17. SECURITY CLASSIFICATION 18. SECURITY CLASSIFICATION 19. SECURITY CLASSIFICATION OF REPORT OF THIS PAGE OF ABSTRACT Unclassified Unclassified Unclassified Unlimited

14. SUBJECT TERMS

15. NUMBER OF PAGES